Design of a Solar Seawater Battery System to increase the Voltage Efficiency of a Seawater Battery

Jinho Lee

Department of Energy Engineering
(Battery Science and Technology)

Graduate School of UNIST

Design of a Solar Seawater Battery System to increase the Voltage Efficiency of a Seawater Battery

A thesis/dissertation
submitted to the Graduate School of UNIST
in partial fulfillment of the
requirements for the degree of
Doctor of Philosophy/Master of Science

Jinho Lee

06/10/2019

Approved by

Advisor

Prof. Youngsik Kim

Design of a Solar Seawater Battery System to increase the Voltage Efficiency of a Seawater Battery

Jinho Lee

This certifies that the thesis/dissertation of Jinho Lee is approved.

06/10/2019

signature

Advisor: Prof. Youngsik Kim

signature

Prof. Yunseok Choi

signature

Prof. Ji-Wook Jang

Abstract

Seawater batteries are promising ESS devices that are competitive in terms of theoretical energy density and cost. However, improving the low voltage efficiency caused by the large overpotential of the oxygen evolution reaction and the oxygen reduction reaction (OER/ORR) remains a challenge that hinders practical and large-scale applications. Here we present a solar-assisted rechargeable seawater battery that integrates TiO_2 nanorods photoanode and a seawater battery within a single device. It is charged to a reduced voltage through photoelectrochemical (PEC) water oxidation of TiO_2 nanorods photoanode, and it is is discharged at a relatively high voltage through the ORR using the heated carbon felt. The charging voltage of the integrated device is greatly lowered, from ~3.78 V to ~2.59 V, with the help of harvested solar energy integrated with the PEC component instead of a carbon current collector; its discharge voltage is ~2.80 V using a carbon current collector. By reducing the charging voltage, we achieved a voltage efficiency of ~108 % at 0.1 mA/cm^2.

Contents

List of Figures

List of Tables

1. Introduction

1.1. Importance of Energy Storage System (ESS)

There is a growing interest in renewable energy sources (solar, wind, geothermal energy, etc) to address negative global environmental issues such as pollution, global warming, and climate change.[1-4]

Harvesting solar energy is one of the strongest, most efficient, and environmentally friendly solutions (Figure 1).[5-9] Solar energy is expressed an eternal and potent energy source, available with operating prices, and waste materials are not yielded. The Earth's surface receives about 100,000 TW of energy from the Sun every hour.[10, 11] It is more than the energy consumption of all human population in a whole year.

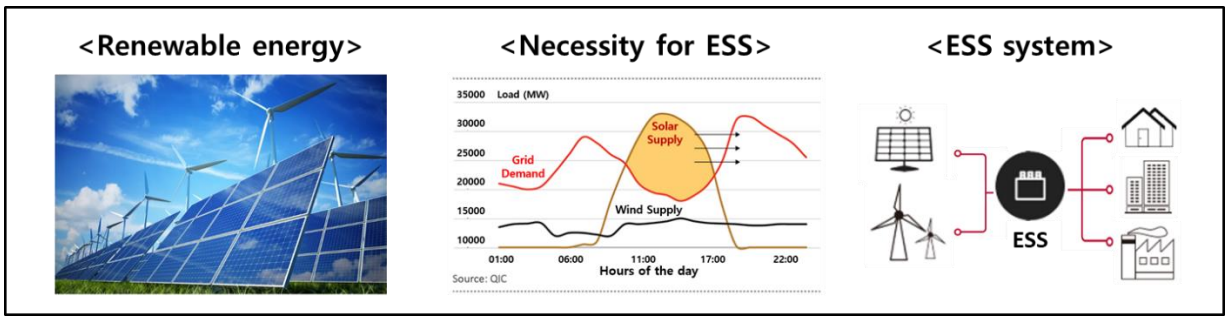

Figure 1. Usage of solar energy with an ESS[12, 13]

However, the availability of solar power for harvesting varies remarkably. No power is available during the night hours, and significant changes occur seasonally because of the changing daylight duration, and on shorter periods due to changing cloud cover and other climate patterns. Overall, this has been a major challenge for both practical and large-scale exploitation of solar power.[1, 14]

In order to harvest solar energy effectively when needed, a system analogous to natural photosynthesis could be utilized. By photosynthesis, solar energy is captured and stored through chemical bonds; similarly the energy captured by photovoltaic (PV) cells could be stored, and then supplied as electricity when needed. To do so, energy storage systems (ESSs) connected to PV cells are becoming widely used.

Among various ESSs, rechargeable batteries are expected to gain a primary role in the future carbon-free, sustainable energy supply.[1-4, 14-15] Li-ion batteries (LIBs) are the most widely used ESSs in

various fields, such as electric vehicles, portable electronics, and grid energy storage.[16]

State-of-the-art LIBs feature a high energy density (≈260 Wh/kg) at the cell level. The material cost of commercialized LIBs accounts for 60% of the total price, and the cathode material (Lithium, Cobalt etc.) accounts for about 40% (Figure 2).

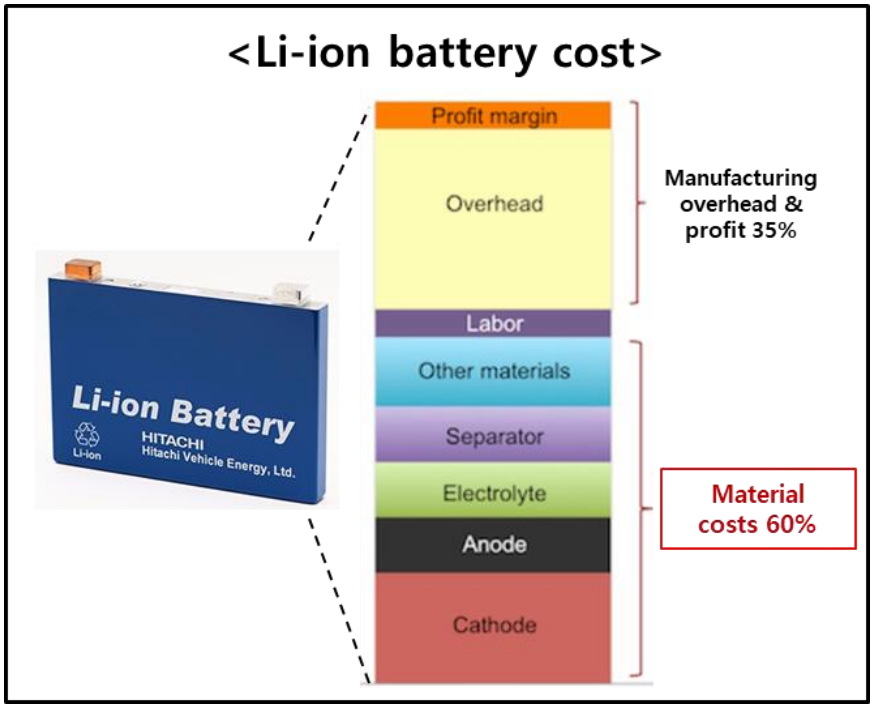

Figure 2. Components of the cost of a Li-ion Battery[17]

Currently, as the market share of electric vehicles grows around the world, the price of lithium is skyrocketing due to the increase in demand for LIBs (Figure 3).

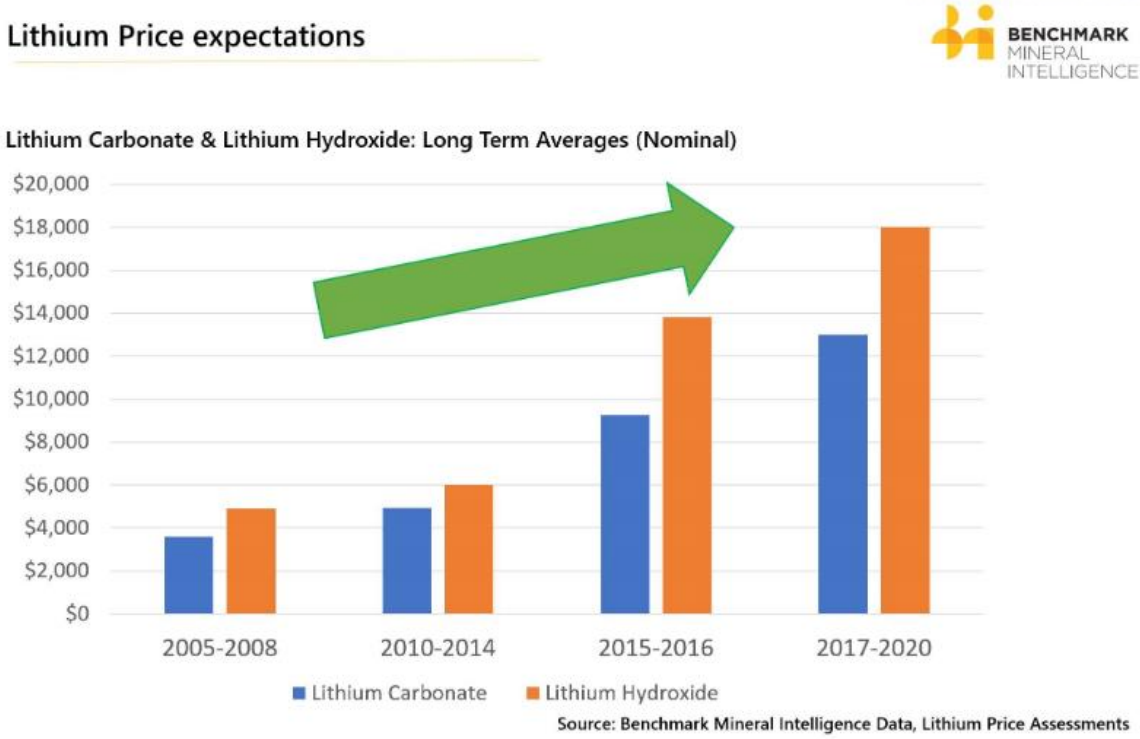

Figure 3. Lithium price expectations[18]

1.2. Seawater battery (SWB)

1.2.1. Introduction

Recently, our group has developed a new type of rechargeable battery, the “seawater battery” (Figure 4).[19-37]

The SWB uses seawater, which is abundant and eco-friendly, as the active material.

SWBs store and supply energy through the redox reaction of water at the cathode side, and the redox reaction of Na at the anode side when charging and discharging.

The use of natural seawater in SWBs can solve the cost of cathode materials, which accounts for a large portion of the material cost of the existing LIBs.

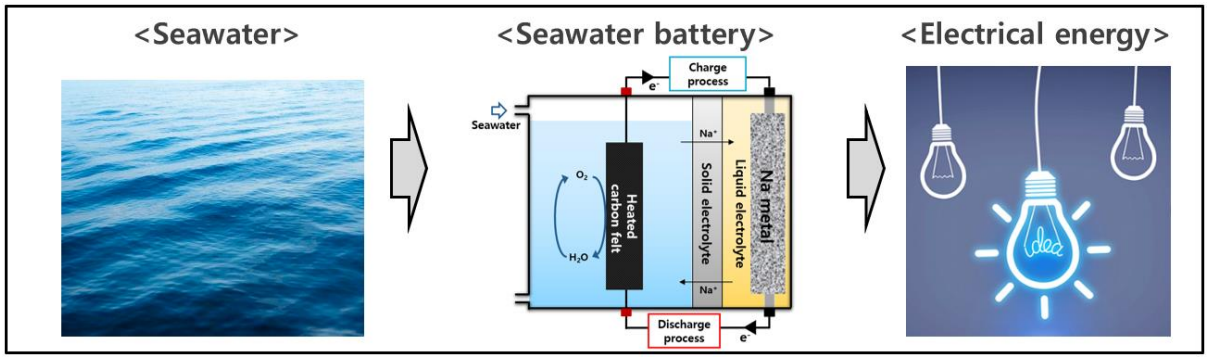

Figure 4. Introduction to SWBs

In the seawater cell, only the anode part, composed of the organic electrolyte and the active material, is sealed, whereas the cathode part has an open structure; thus, theoretically, the Na ions (the active material) can be supplied indefinitely (Figure 5).[38]

For these reasons, SWBs are more competitive than conventional batteries in terms of environmental impact, energy density[38], and price.

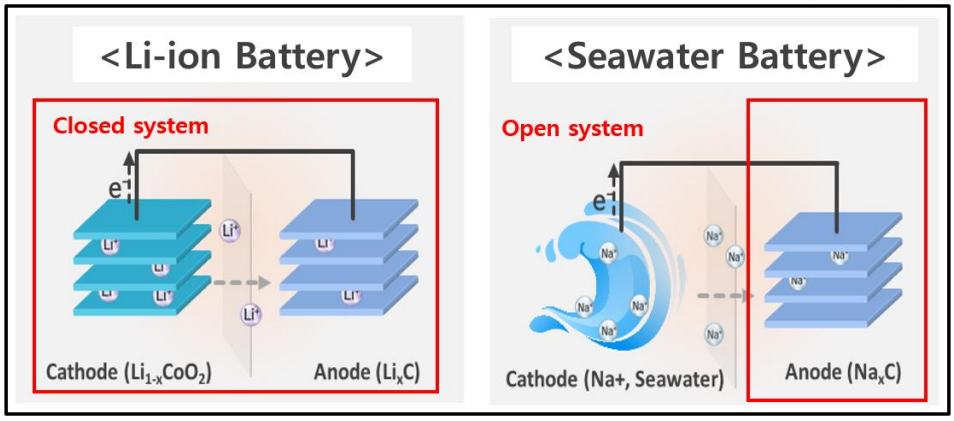

Figure 5. Difference between LIB and SWB[39]

1.2.2. Cell configuration and mechanism of the SWB

Figure 6 shows the cell configuration of the SWB.

The SWB is physically divided by a solid electrolyte in the cathode and anode parts. The current collector is immersed in seawater. Therefore, the material the collector is composed of should be chemically stable in seawater (Table 1).[38]

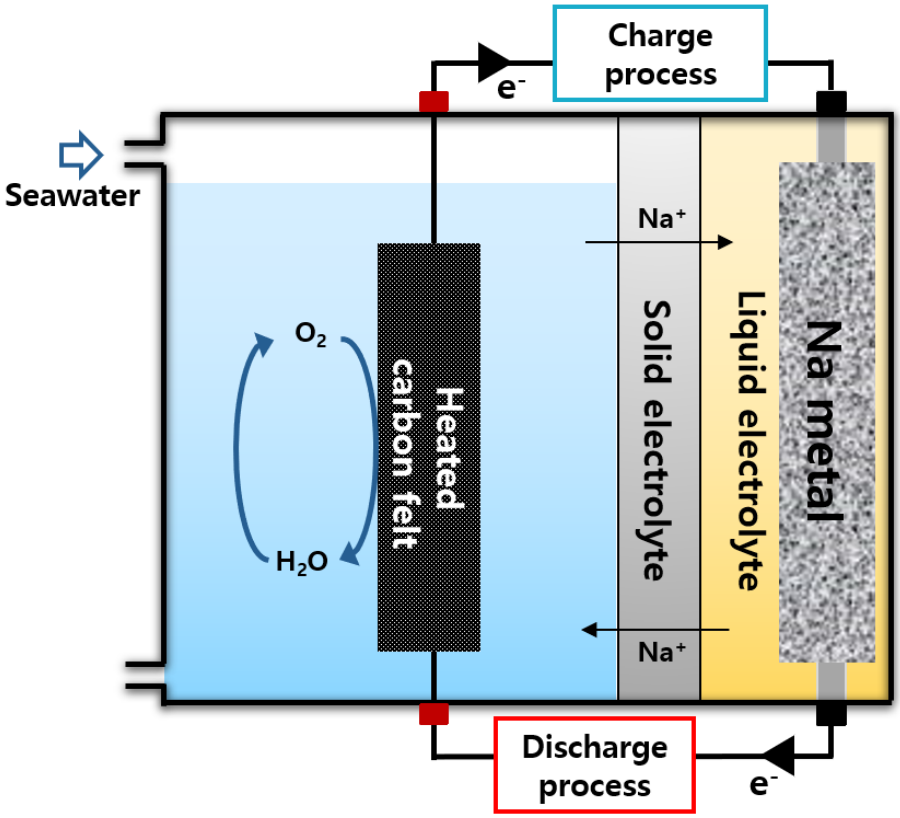

Figure 6. The cell configuration of the SWB

The cathode part of the SWB consists of seawater, a collector, and a catalyst. Seawater contains Na ions, which are the active material. The current collector not only provides reaction sites where the cathode reaction occurs, but also serves as a passage through which electrons can move to the anode side. The role of the catalyst is that to improve the kinetic of cathode reactions and properties.

The solid electrolyte must be selectively permeable to the Na ions, and physically interposed between the seawater and the organic electrolyte, therefore it should not react with the aqueous and non-

aqueous materials. NASICON ($Na_{1+x}Zr_2Si_xP_{3-x}O_{12}$), which is a solid electrolyte satisfying these conditions, has been chosen to serve this purpose.[38]

The anode part consists of the active material immersed in an organic electrolyte.

The mechanism of charge/discharge of the SWB is as follows.

The oxygen evolution reaction (OER), the oxygen reduction reaction (ORR), and the redox reaction of seawater occur in the cathode part (Equation 1).

The electrons generated by the reaction move to the anode through the external circuit.[38] At the same time, Na ions selectively move to the cathode through the NASICON (Equation 2).

In the anode par, the redox reaction of Na occurs, which uses the transferred electrons and Na ions.

The overall reaction is presented in Equation 3. The theoretical cell voltage is 3.48 V (Na^+/Na) at pH 8.[38]

Cathode reaction

$$O_2\,(aq) + 2H_2O\,(l) + 4e^- \leftrightarrow 4OH^-;\ E°= 0.75\ V\ vs\ NHE\ (pH = 8) \quad (1)$$

Anode reaction

$$Na^+ + e^- \leftrightarrow Na\ (s);\ E°= -2.71\ V\ vs\ SHE \quad (2)$$

Overall reaction

$$4Na\ (s) + O_2\,(aq) + 2H_2O\,(l) \leftrightarrow 4NaOH\ (aq);\ E_{cell} = 3.48\ V\ vs\ Na^+/Na\ (pH = 8) \quad (3)$$

	Component
Cathode part	Seawater • Including active material Current collector • Reaction sites for the cathode reaction • Electron paths Catalyst
Solid electrolyte	NASICON (Na Super Ion Conductor, $Na_3Zr_2Si_2PO_{12}$) • Selective pathway, only for Na ions
Anode part	Active material (Na metal) Non-aqueous electrolyte

Table 1. Components of the SWB

1.2.3. Cathode current collector of the SWB

Among the components of the SWB, the cathode current collector serves as a reaction channel for the anode reaction, as well as an electron transfer path. By improving the current collector in the cathode part, the voltage efficiency and cycle stability of the SWB can be improved.

In order to achieve these goals, the cathode current collector needs to be hydrophilic, to have good catalytic properties, and to have a large specific surface, electrical conductivity, and chemical stability.

As demonstrated in Table 2, the properties of carbon-based materials make them suitable to serve as collectors. We investigated various commercial carbon-based fabrics applied to the SWB, such as Carbon felt, carbon cloth, carbon paper, and so on.

Product name (Manufacturer)	**Specific surface area (m^2/g)**	**Functional groups**	**Voltage gap**
Carbon felt (CNF co. Ltd)	0.62	C: 93 %, O: 4.9 %	-
Carbon cloth (Sigmatech co. Ltd)	0.30	C: 75 %, O: 19 %, N: 5 %	-
ACC-5092-20 (Kynol co. Ltd)	≈2000	C: 96 %, O: 5 %	0.54 V
ACC-5092-10 (Kynol co. Ltd)	800	C: 85 %, O: 12 %, N: 3 %	0.76 V
ACC-5092-15 (Kynol co. Ltd)	1300	C: 95 %, O: 5 %	0.61 V
STF-1800 (Sutong co. Ltd)	1800	C: 92 %, O: 8 %	0.43 V

Table 2. Characteristics of various commercial carbon-based fabrics

Among the considered materials, Carbon felt (CNF co. Ltd) has the best performance in the SWB, and has been taken as a reference material.

As a downside, carbon-based materials generally have poor hydrophilicity because they use polymeric sizing agents to increase their mechanical strength.

To overcome this limitation, Carbon felt was heated at 500 °C for 2 hours in an air atmosphere to generate functional groups on the surface that improve hydrophilicity, such as C – O and C = O bonds, and surface area (from 0.62 m^2/g to 2.23 m^2/g).[38]

Using this heated Carbon felt (HCF), the charge and discharge voltage profile of the SWB could be lower than that evaluated using pristine Carbon felt.

1.2.4. Limitations of the SWB

The cathode part of the seawater battery has an issue. Due to the sluggish kinetic of the OER and ORR, the charge and discharge processes of the SWB is accompanied by a large overvoltage (Figure 7). Therefore, the voltage profile of the seawater battery has a wide voltage gap, which means that the voltage efficiency is low. This implies that not all of the electrical energy used during charging can be retrieved during discharging, and is an undesirable feature, given that the purpose of the ESS is that to store energy and use it when needed.

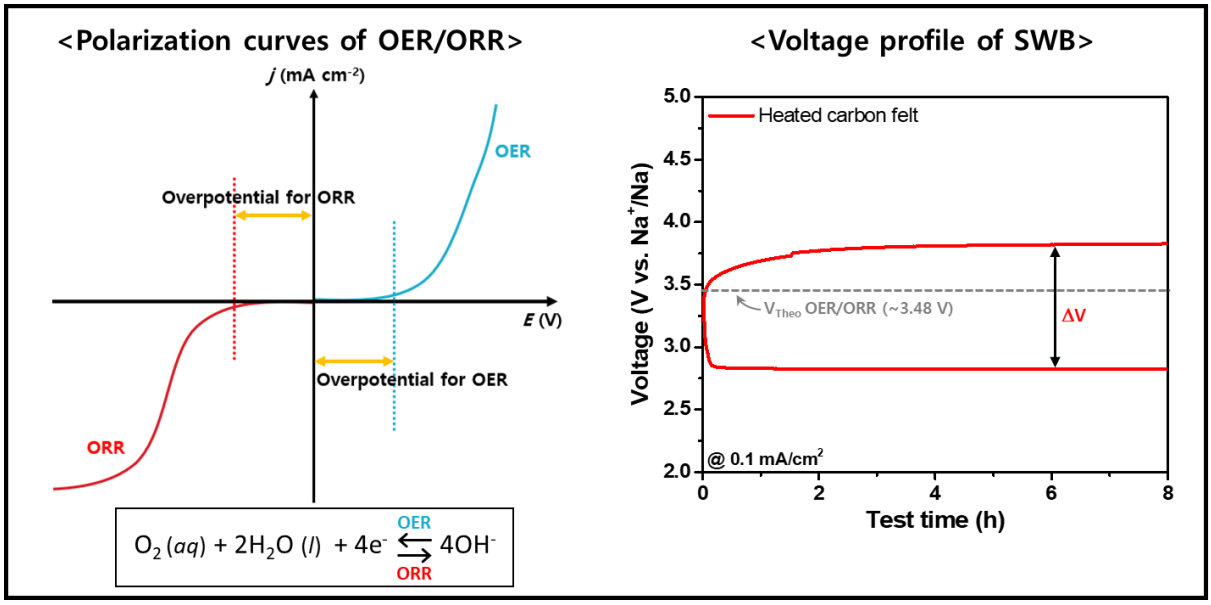

Figure 7. Polarization curves of OER/ORR and voltage profile of the SWB

1.3. Photoelectrode

1.3.1. Introduction

Using renewable energy effectively is essential for reducing CO_2 emissions and developing a sustainable society that does not depend on fossil resources.[10, 40] The use of solar energy is very significant, yet technological limitations exist that hinder an optimal utilization.[42]

Artificial photosynthesis is the most recent technology for harvesting solar energy that has been developed. Among the existing artificial photosynthesis technologies, the photoelectrochemical water splitting technology (PWST) produces hydrogen and oxygen directly by splitting water molecules, using photocatalysts or photoelectrodes. These are made by oxide semiconductors, which can be synthesized easily.

The PWST is cost-effective and has been studied extensively. It is a candidate for serving as a fundamental technology in a future hydrogen-based society.

The PWST for the production of solar fuel has been attracting interest since 1972, when the n-type TiO_2 by Honda and Fujishima has been reported (Figure 8).[43-45] This is in line with the growing need for renewable non-carbon energy production.

This PWST has grown tremendously through several reports describing many strategies to improve solar-to-hydrogen (STH) efficiency.[46] The reports stressed that the development of the PWST requires a better understanding of the mechanistic features of the photoelectrochemical water splitting reaction.[46-64]

However, even though some impressive progress has been made in the PWST, the large-scale application of this technology still remains difficult.[65-68]

A relatively simple explanation of the working mechanism of the PWST is as follows: the adsorption of photons by photoelectrodes leads to the generation of charge carriers, the photo-generated holes (h^+), and the photo-excited electrons (e^-). As a result of the photoelectrochemical water splitting generated from the results assembled from techniques *(in-situ),* these photo-generated holes (h^+) and photo-excited electrons (e^-) finally move from the bulk to the surface of the photoelectrode to generate intermediate species.

Electron-hole pairs play a key role in decreasing the activation energy for the photoelectrochemical water splitting reaction, which is the reason why the solar rechargeable battery can increase the voltage efficiency.[69]

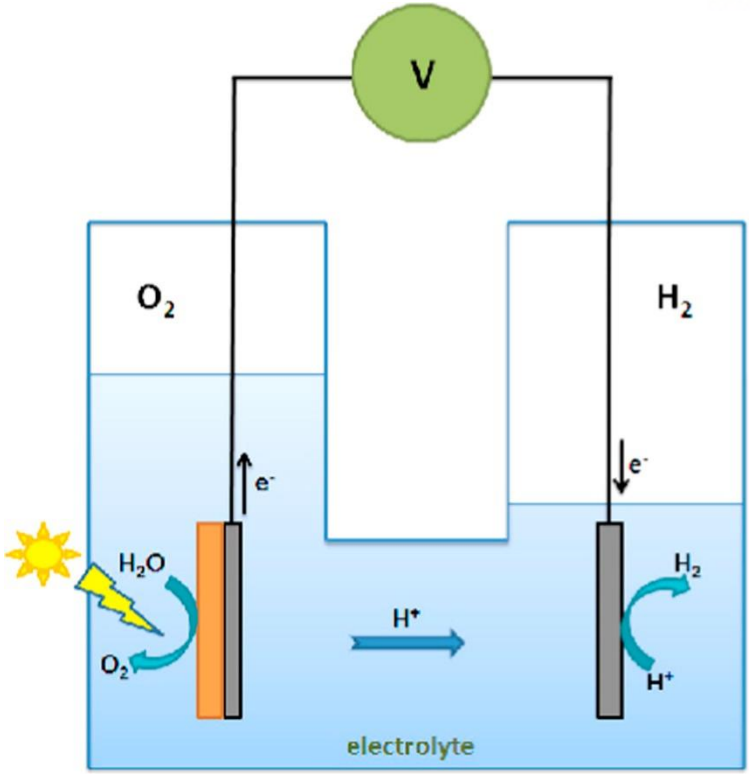

Figure 8. Schematic diagram of a photoelectrochemical water splitting cell[70]

1.3.2. Photoanode

The photoanode is the location where the oxygen generating reaction occurs. The photoanode should refer to n-type semiconductors, so that the electric field which is produced by the band bending on the interface can operate the photo-generated holes on the surface of the photoanode. The photoanode material should also have an appropriate band gap and band position between the valence band and conduction band.[71]

The appropriate band gap and band position should be chosen according to its application in a single or multiple band gap system, and to their electrical properties.

Moreover, these materials need to maintain a constant state under the oxidation of water conditions, and if the surface kinetic of the OER is rate-limited, the OER catalyst should be put on the photoelectrode surface.

Upon photo-excitation and charge separation of n-type semiconductors, photo-generated holes in the valence band spread to the photoanode-electrolyte interface for the oxidation of water. The difference between the oxygen-placed valence band at ~3.0 V and the potential of the oxygen evolution reaction at 1.23 V vs NHE is ~1.77 V. The surface kinetic is a main problem for enhancing the performance of photoanode materials.

Thermal relaxation wastes most of the ~1.77 eV absorbed in the oxide. Few semiconductors meet the demands of electronic structures and stability required for photoanodes. Thus, in most cases, photoanodes switch solar energy to oxygen at comparatively low efficiency.[71]

1.4. Previous research

1.4.1. Electro-catalysts

To solve this voltage efficiency problem, our group investigated the Pt/C electro-catalyst, which is well known for improving the kinetic of the ORR, and Ir, which has been reported to improve the kinetic of the OER.

However, Ir and Pt are costly catalysts due to precious metals.[72-75]

Nonetheless, we applied Ir and Pt to the cathode current collector.

In addition, we have also applied Cobalt Manganese Oxide, which is a non-precious metal-based catalyst.[27]

Figure 9 shows the charge-discharge voltage profile of the SWB by applying Ir, Pt, or CMO as a secondary working electrode catalyst.

These catalysts improved the surface kinetic of the OER/ORR.

The OER/ORR are the redox reactions at the cathode part of the SWB. We observed a fairly high voltage efficiency for Ir/C (≈80.3 %), Pt/C (≈83.1 %), and CMO (≈84.4 %) in comparison to that of the bare HCF (≈72.7 %).

However, this efficiency is still low compared to that of existing LIBs which use $LiFePO_4$ as the anode material (Table 3).[76]

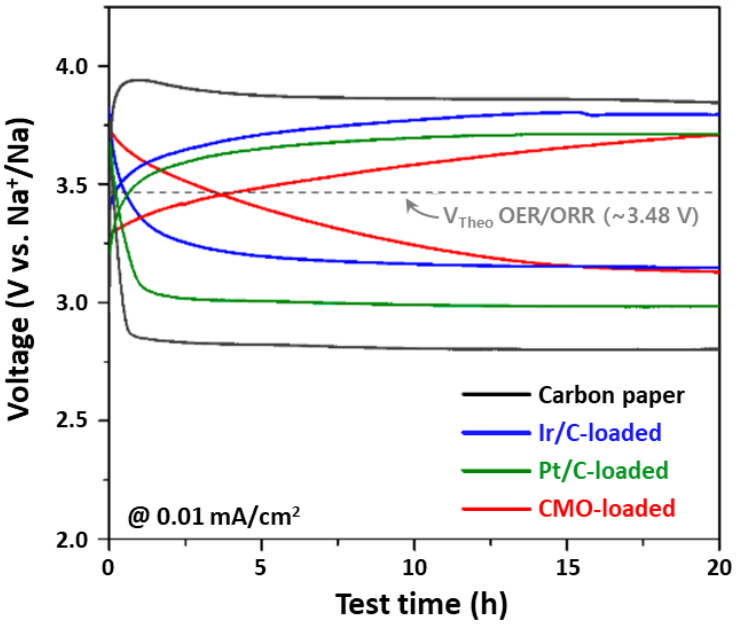

Figure 9. Voltage profile of the SWB with various electro-catalysts[27]

	Voltage Efficiency
Carbon Paper	72.7 %
Ir/C-loaded	80.3 %
Pt/C-loaded	83.1 %
CMO-loaded	84.4 %
Li-ion Battery	96.5 %

Table 3. Voltage efficiency of the SWB with various electro-catalysts, and of the LIB

1.4.2. Solar rechargeable battery (SRB)

Another way to increase the voltage efficiency is to use a solar rechargeable battery (SRB) system that integrates a photoanode and a battery into a single device.[78-82]

SRB harvest solar energy to generate electricity, which is deposited in a combined storage directly. An SRB is composed of a photoanode, a counter electrode, and charge storage electrode (Figure 10).

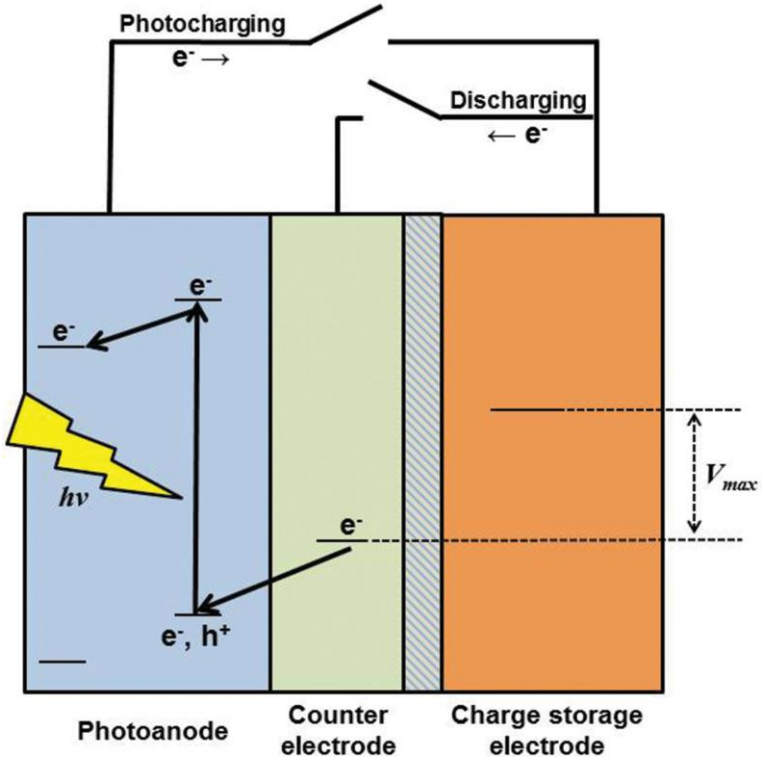

Figure 10. Scheme of a Solar rechargeable battery[77]

Under illumination, solar energy is absorbed by the photoanode, and charge carriers (electron-hole pairs) are excited by solar energy. Electrons move to charge the storage electrode, and are deposited in the electrode. The electrons of the counter electrode will counterbalance the holes in the photoanode, and the electrons will charge the device. The electrons move back from the charge storage electrode to the counter electrode during the discharge process. The counter electrode is divided by a membrane from the charge storage electrode, and provides the counterbalance by means of cations.[77]

This system uses a strategy to store the electrical energy of the charging process that entails the

photoanode that can use sunlight.

Figure 11 shows the cell configuration of the SRB and its voltage profile.

The SRB, a unit that combines photoanode and a battery, has two distinct electrodes in the cathode part for charging and discharging.

The photoanode serves as the cathode during the charging process, whereas the heated carbon felt, which is the existing battery cathode, is used during the discharging process.

Photoanodes refer to semiconductors, in which the light is absorbed to generate electron-hole pairs.

Studies on the SRBs have recently been reported. Figure 11 presents an example of an SRB system. The graph shows that the charge voltage reduced from 3.45 V to 2.78 V at a current density of 0.02 mA/cm^2 when using the photoanode.

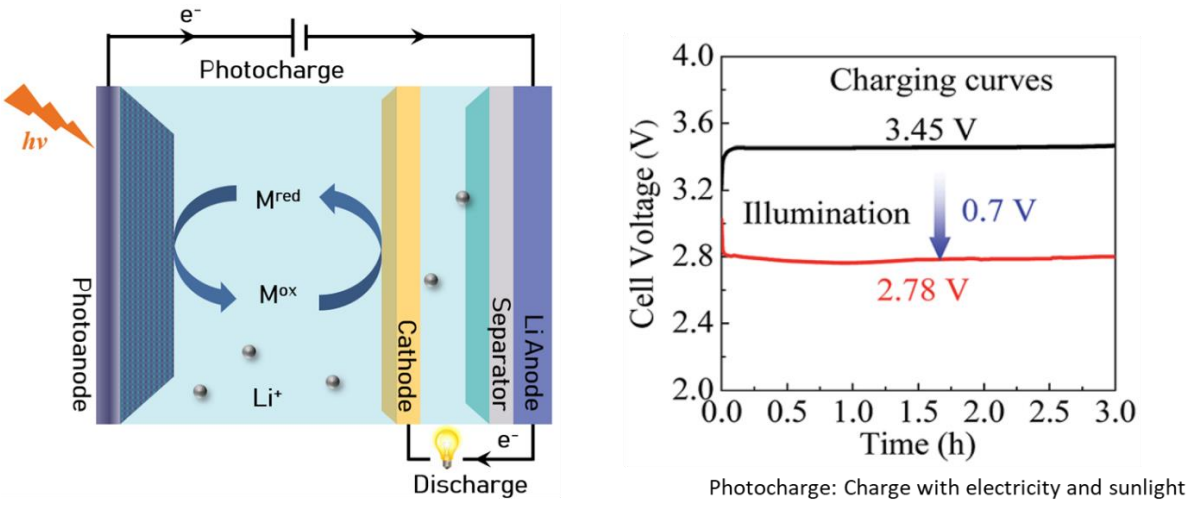

Figure 11. Scheme of a solar rechargeable Li-ion battery and its voltage profile[72]

1.5. Research proposal

To overcome the voltage efficiency issue of the SWB, we designed a solar seawater battery (SSB) of a hybrid type that integrates a photoanode and the SWB within a single device by benchmarking the SRB (Figure 12).

The SSB uses 3 electrolyte systems: a solid electrolyte, an aqueous liquid electrolyte, and a non-aqueous liquid electrolyte.

In the SSB, we use NASICON ($Na_3Zr_2Si_2PO_{12}$), which is the same solid electrolyte as that used in the SWB. Aqueous (seawater) and non-aqueous liquid electrolytes also are the same as in the SWB.

The anode part and the solid electrolyte of the SSB are the same as those of the SWB, but the cathode consists of two separated electrodes for the OER and the ORR.

Because the other cathode is used for charging and discharging, two channels are required in the cycle stability test.

Therefore, the galvanostatic cycle tests performed in the SSB uses two channels to separate and cycle independently the photoanode for the OER, and the heated carbon felt for the ORR.

We expect to increase the voltage efficiency of the SWB by reducing the charging voltage through this design.

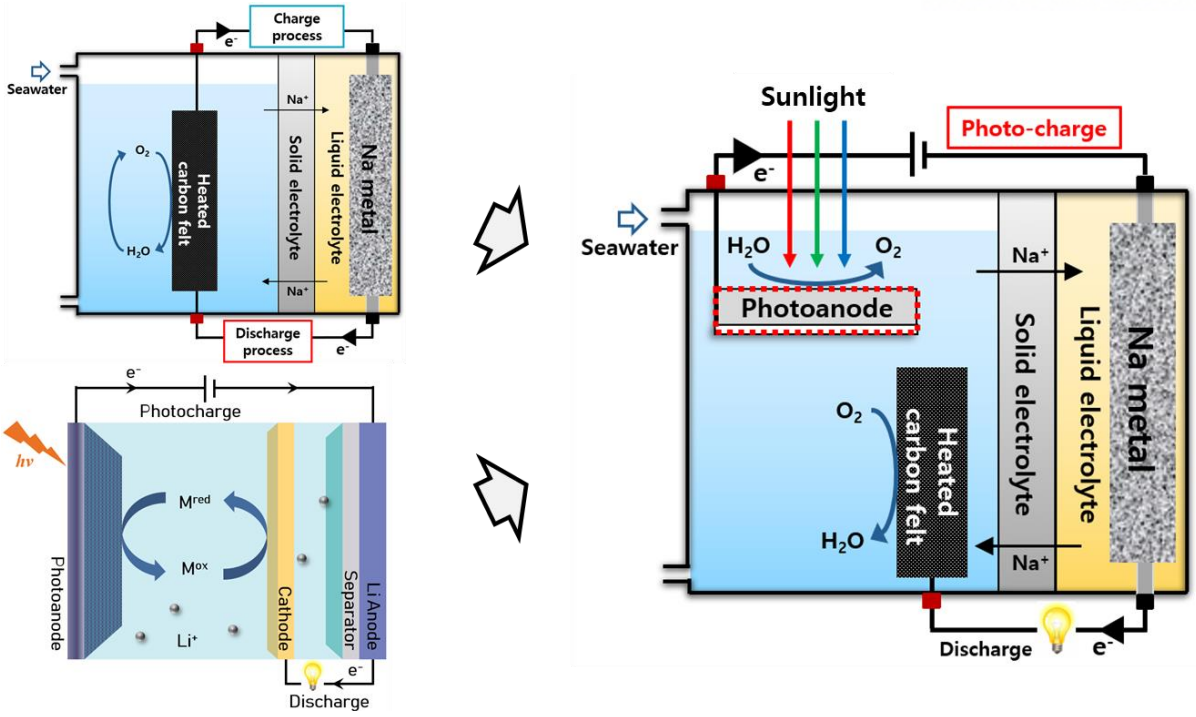

Figure 12. Solar seawater battery which is the integration of the photoanode and seawater battery by benchmarking the solar rechargeable battery

2. Results and Discussion

2.1. Cell configuration of Solar seawater battery

Figure 12 shows the cell configuration of the solar seawater battery.

Solar seawater battery uses three electrolytes system which consists of NASICON (solid electrolyte) inserted between aqueous liquid electrolyte and non-aqueous liquid electrolyte.

The anode part is composed of Na metal immersed in non-aqueous liquid electrolyte. And solid electrolyte of the solar seawater battery uses NASICON which is the same as those of the seawater battery, but cathodes consist of two separated electrodes for oxygen evolution reaction and oxygen reduction reaction which are redox reaction of solar seawater battery.

One is the photoanode for photo-charging (oxygen evolution reaction) and the other is the heated carbon felt for discharging (oxygen reduction reaction).

When solar seawater battery is below the charging process, the anode is connected with photoanode for reducing the charge voltage compared to the heated carbon felt (the existing seawater battery cathode) by using solar energy. Compared to the charging process, the anode is connected with the heated carbon felt.

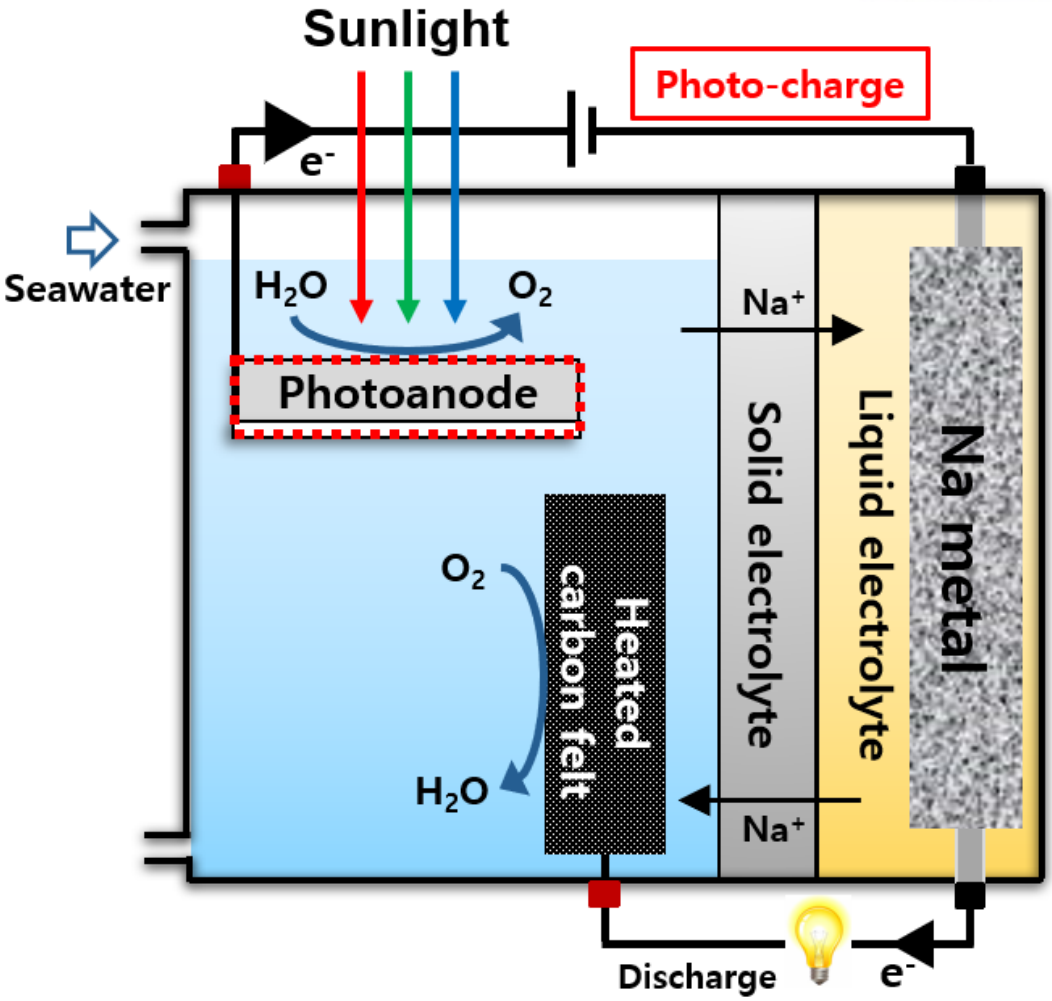

Figure 13. Schematic illustration of the cell configuration of solar seawater battery

2.2. Mechanism of Solar seawater battery

As mentioned in chapter 1.2.2 (Cell configuration and mechanism of SWB), the theoretical charging voltage of the seawater battery is the difference between the potential of the cathode and anode reaction.

But it is different from the mechanism of the solar seawater battery.

Figure 13 shows the difference of the mechanism between seawater battery and solar seawater battery.

Upon illumination, the photon captured by the photoanode makes electron-hole pairs. And the photo-generated holes in the valence band transfer to the Photoanode/seawater interface, oxidizing seawater to O_2. Meanwhile, the photo-excited electrons in the conduction band edge flow toward the anode through the external circuit, which decreases the charging voltage, as much as the energy difference between the conduction band of the photoanode and the potential of water oxidation in seawater.

Through this mechanism, the photo-charging voltage can be lower greatly due to the solar energy input.

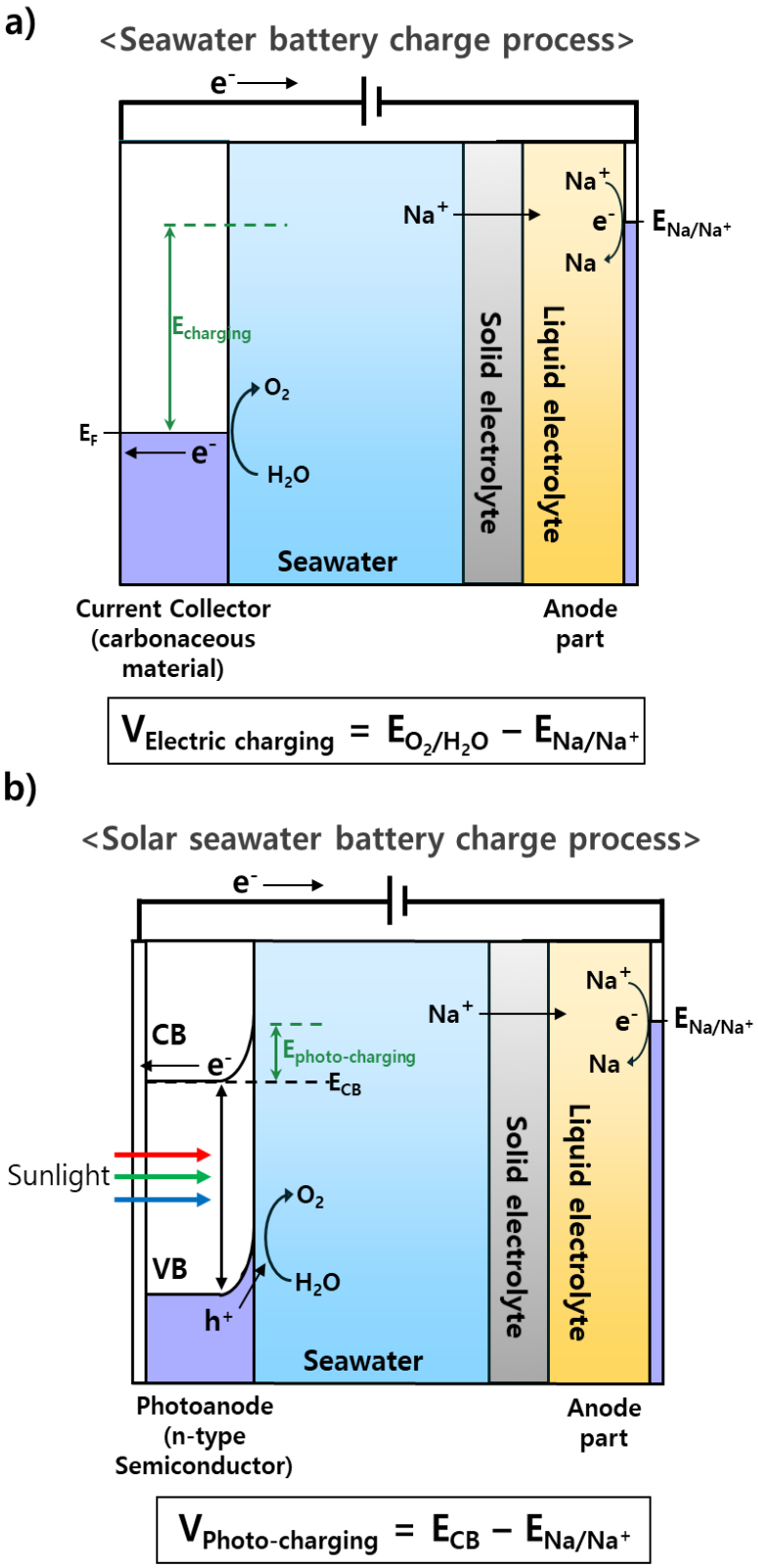

Figure 14. The difference mechanism between a) seawater battery and b) solar seawater battery

2.3. Design of SSB cell tester

To implement the system practically, to optimize the cell design and configuration is important for efficient photo-charging and discharging. The purposes of designing the system tester is to maximize the performance of the system, create a uniform experimental environment, and identify the properties of the material itself within the cell system.

To maximize performance and identify the properties of a material itself, it is necessary to identify external variables that affect system performance and to eliminate external variables.

Experimental results show that the shape of the tester water tank, the position of the photocatalyst, and the stirring speed affect the performance as external variables.

We compared the shape of the tester tank (Figure 14a). As a result of the comparison, the photocurrent characteristics in the circle shaped water tank were better than the photocurrent characteristics in the rectangle shaped water tank. I think that because the shape of the water tank is round, the seawater containing active materials can flow smoothly. In order to smooth the flow of seawater, the shape of the tester water tank was made circular shape.

We also compared the differences in characteristics according to the position of the photoanode were compared. We confirmed that the closer the position of the photoanode is to the sea surface, the higher the characteristics are (Figure 14b). I think that the reason is that it is the scattering which occurs when the light penetrates the sea water.

The difference in characteristics according to the distance difference between the photoanode and the seawater coin-type cell was compared (Figure 14c). Experimental results show no difference in performance between the photoelectrode near the sea water cell and the center of the water tank.

Thus, the position of the photoanode was fixed at the center and we designed the solar seawater battery tester by checking and removing these variables (Figure 15).

In the middle of the tester, photoanode is positioned horizontally to absorb enough solar energy.

In addition, the seawater battery coin cell and heated carbon felt were placed close to each other for high discharge performance.

And we fixed the position of the electrodes for uniform experiment.

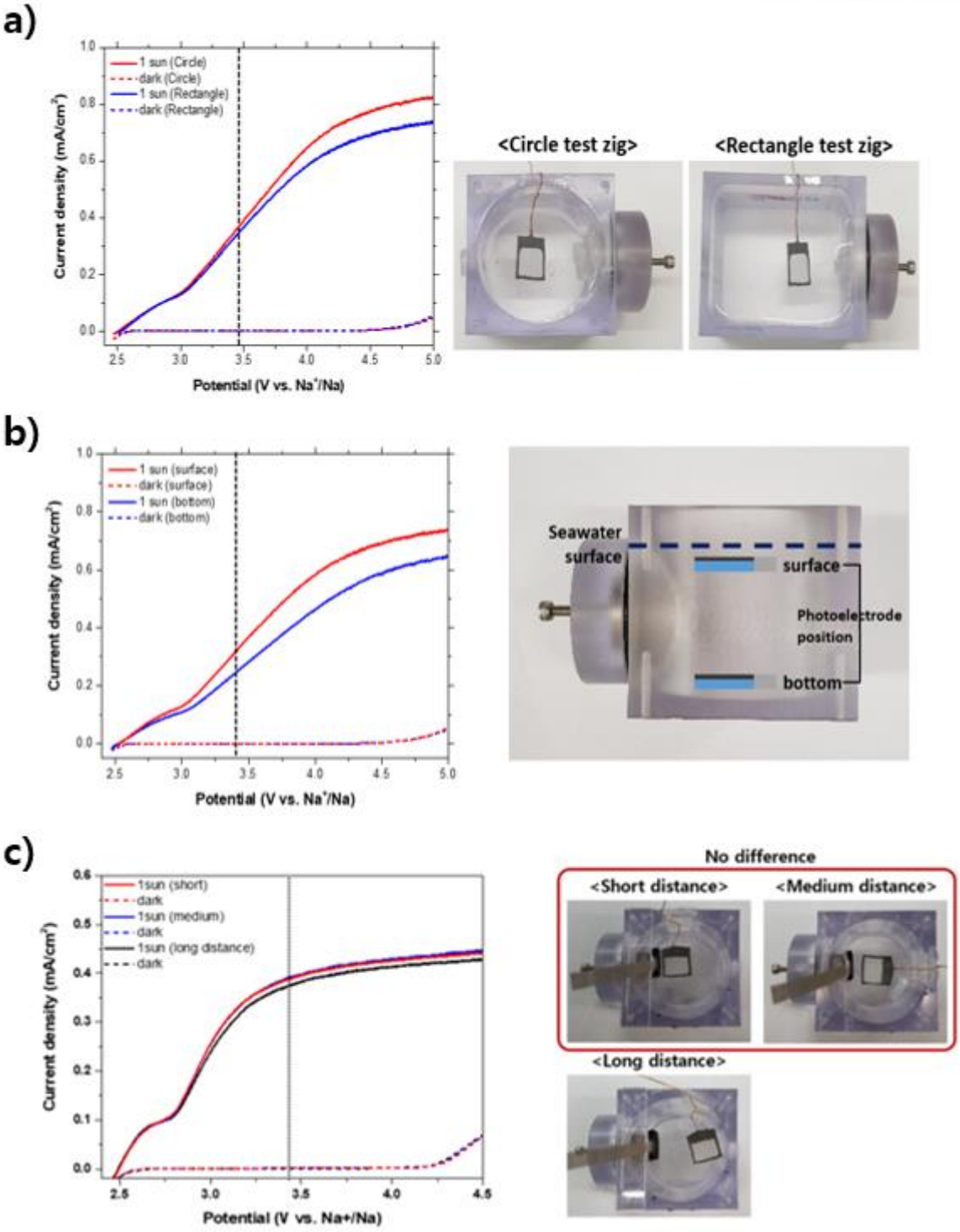

Figure 15. Various external variables affecting the experimental environment; a) The shapes of the solar seawater battery tank; b) the positions of the photoanode; c) the distance difference between the photoanode and the seawater coin-type cell

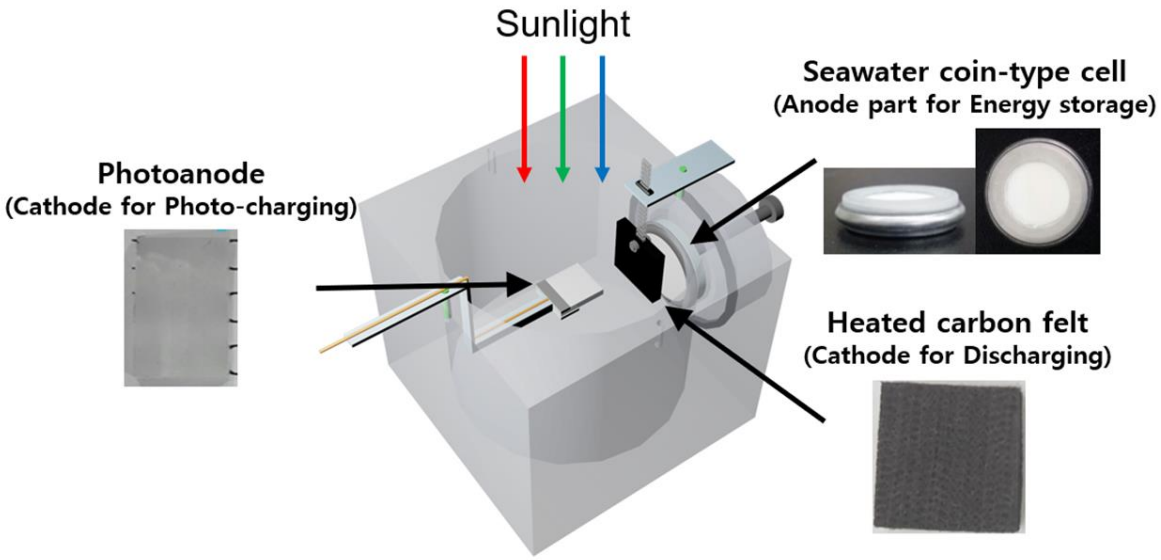

Figure 16. The image of solar seawater battery tester

2.4. Design of Photoanode

Figure 16 shows the band edge positions of photoanode candidates. The band edge positions mean that the valence band for the photo-generated holes and conduction band for the photo-excited electrons.

So, as shown in Figure 16, 0.0 V_{RHE} (the redox reaction of O_2/H_2O) is always contained between the band edge positions of these photoanode material candidates.

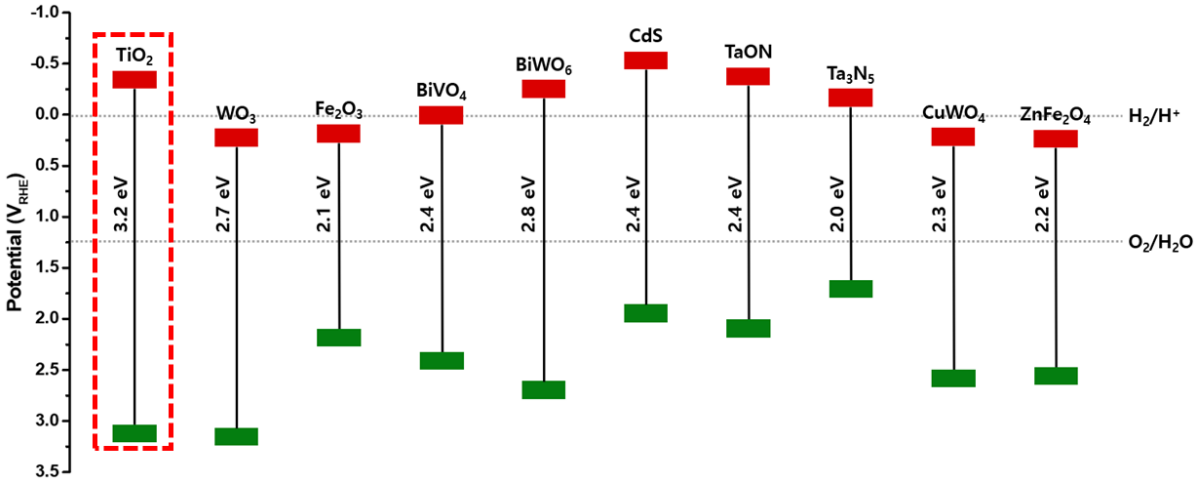

Figure 17. Band edge positions of photoanode candidates

Among these various photoanodes, mainly TiO_2, WO_3, and Fe_2O_3 have been extensively studied for reasons of high resistance to photo-corrosion, chemical stability, nontoxicity, and low cost.[8, 9, 11, 40, 81-86]

Of these candidates, we chose TiO_2 material because it has been studied for the longest time (Honda group) and is commonly used.

And nanostructures have some advantages than the bulk structures.

First, photoelectrodes of nanostructure provide a greatly large surface area for redox reactions to occur, which can expressively increase the efficiency. Second, the electron-hole pairs overlay factor and electron-hole pairs exchange interaction increase significantly due to quantum size restriction in nanomaterials, resulting in increased band-gap energy and increased oscillator strength or absorption coefficient, as compared to bulk structures. Third, the distance for photogenerated holes is reduced

by the small sizes of nanomaterials to diffuse to the photoanode/electrolyte interface for the water oxidation. In this case, the loss via recombination of electron-hole pairs can be decreased, which is specially significant for semiconductors with short hole diffusion length (Figure 17).

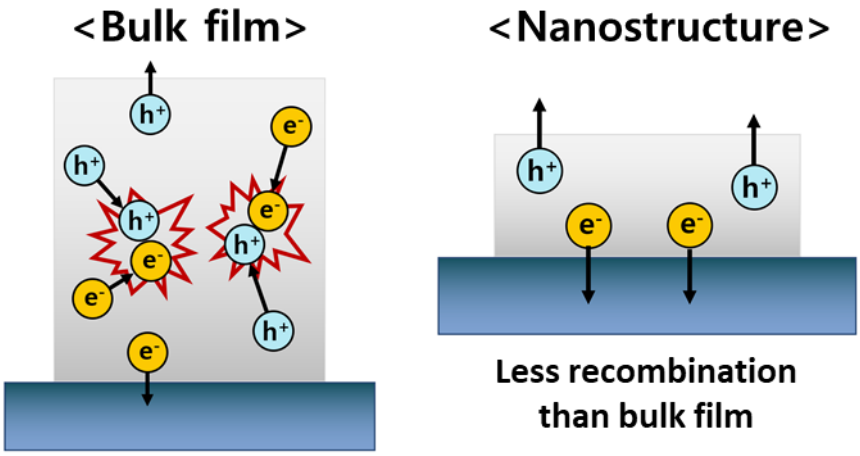

Figure 18. The difference of the distance for photogenerated holes between the bulk film and nanostructure

Fourth, the fundamental optical and electronic properties can be designed and modified through controlled variation of nanomaterial structure. For example, varying semiconductor nanocrystals size to increase the light absorption can tune the band gap of semiconductor nanocrystals in the solar spectrum. Moreover, the separation of electrons and holes would be expressively improved nanostructures if their diameters are similar to the size of the depletion layer. Fifth, the growth of single-crystal nanomaterials on different substrates can be allowed by the unique bottom-up synthetic strategy without the formation of dislocations due to the lattice mismatch between growth substrate and semiconductor.[92]

For these reasons, we selected TiO_2 material and nanorods structure. And we synthesized TiO_2 nanorods on fluorine-doped tin oxide (FTO) substrate using a hydrothermal method (Figure 18).

<Nanorods> <TiO_2 nanorods on FTO>

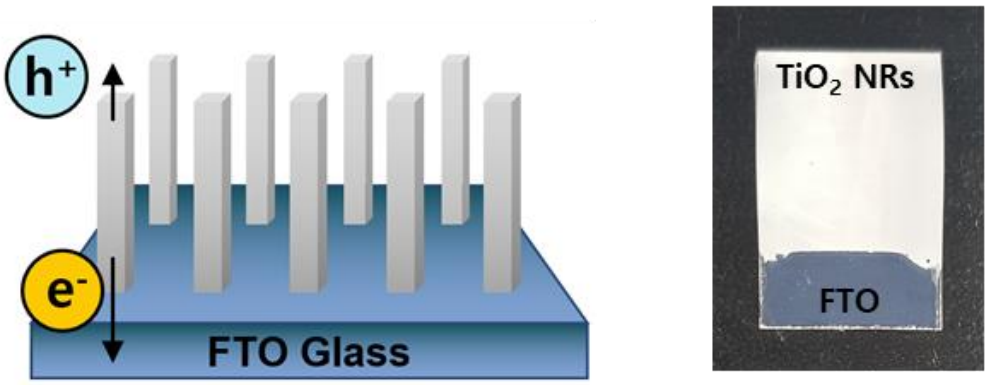

Figure 19. The image of nanorods structure and the picture of TiO_2 nanorods on FTO

2.5. Preparation process of the TiO_2 Nanorods photoanode

The TiO_2 Nanorods was prepared by Titanium (IV) n-butoxide (KANTO chem.) on FTO substrates based on the hydrothermal method, followed by calcination at 450 C for 1 h in air atmosphere. And We follow a series of processes for the preparation of the TiO_2 nanorods on FTO substrate (Figure 19).

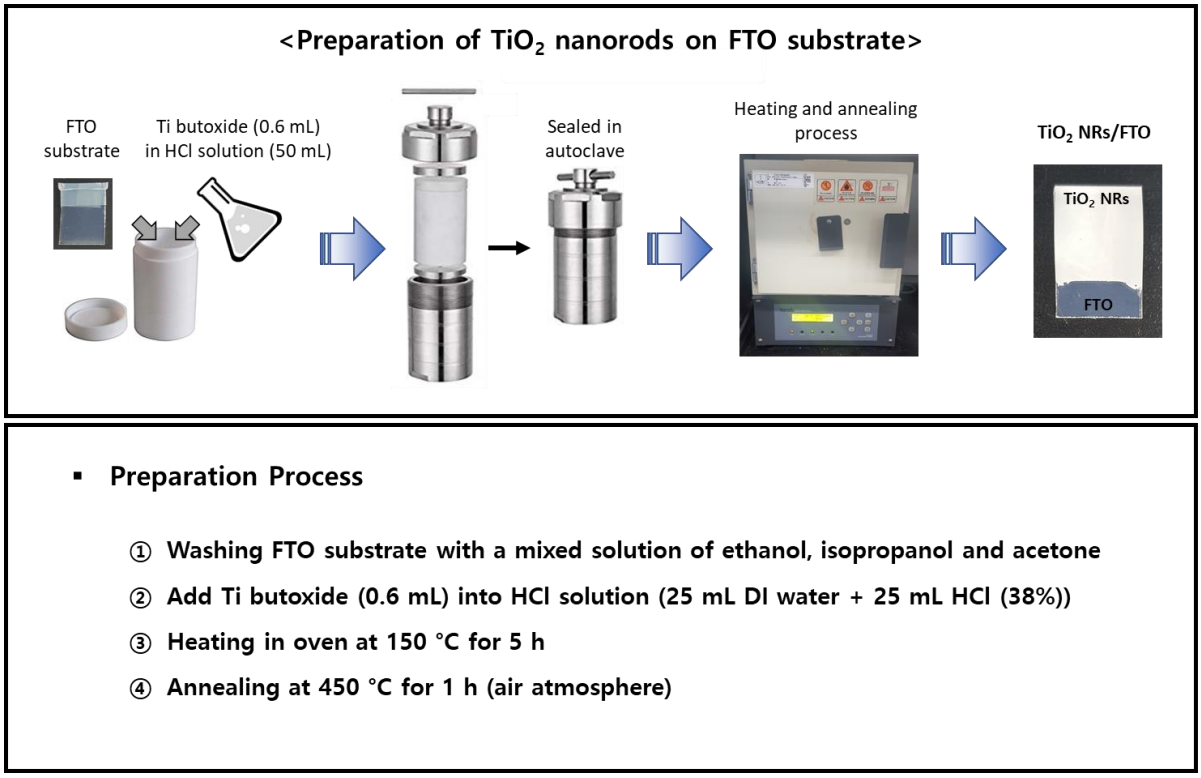

Figure 20. Preparation of TiO_2 nanorods on FTO substrate and its processes

2.6. Characterization of the TiO_2 Nanorods photoanode

We confirmed the photoanode was rutile phase TiO_2 nanorods photoanode grown on FTO substrate. We examined the crystal structure by X-ray diffraction (XRD) analysis. We confirmed that the synthesized TiO_2 was a rutile structure by XRD analysis (Figure 20).

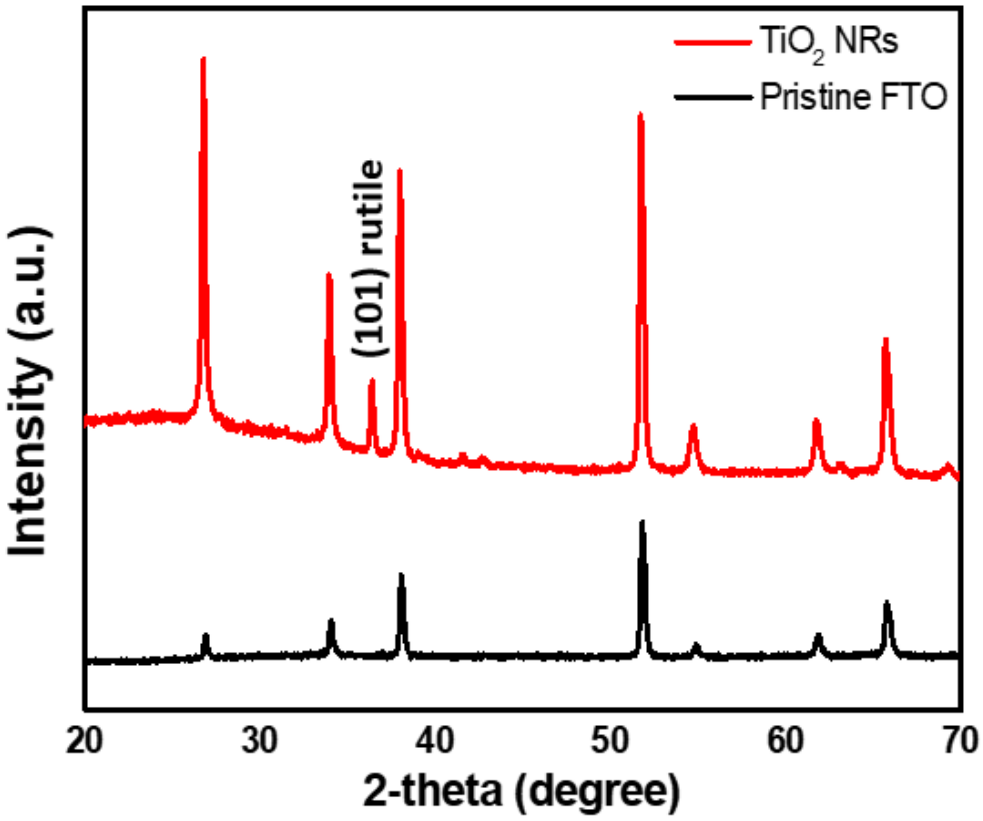

Figure 21. XRD patterns of TiO_2 nanorods photoanode

To investigate the light absorption property of TiO_2 nanorods photoanode, we measured wavelength range from 200 nm to 800 nm by using the ultraviolet-visible (UV-Vis) under illumination (Figure 21). We confirmed that the light is absorbed near 420 nm. This result was consistent with the absorbance value of the rutile phase of the reported paper. So, we confirmed once again that the synthesized TiO_2 nanorods photoanode is in the rutile phase.

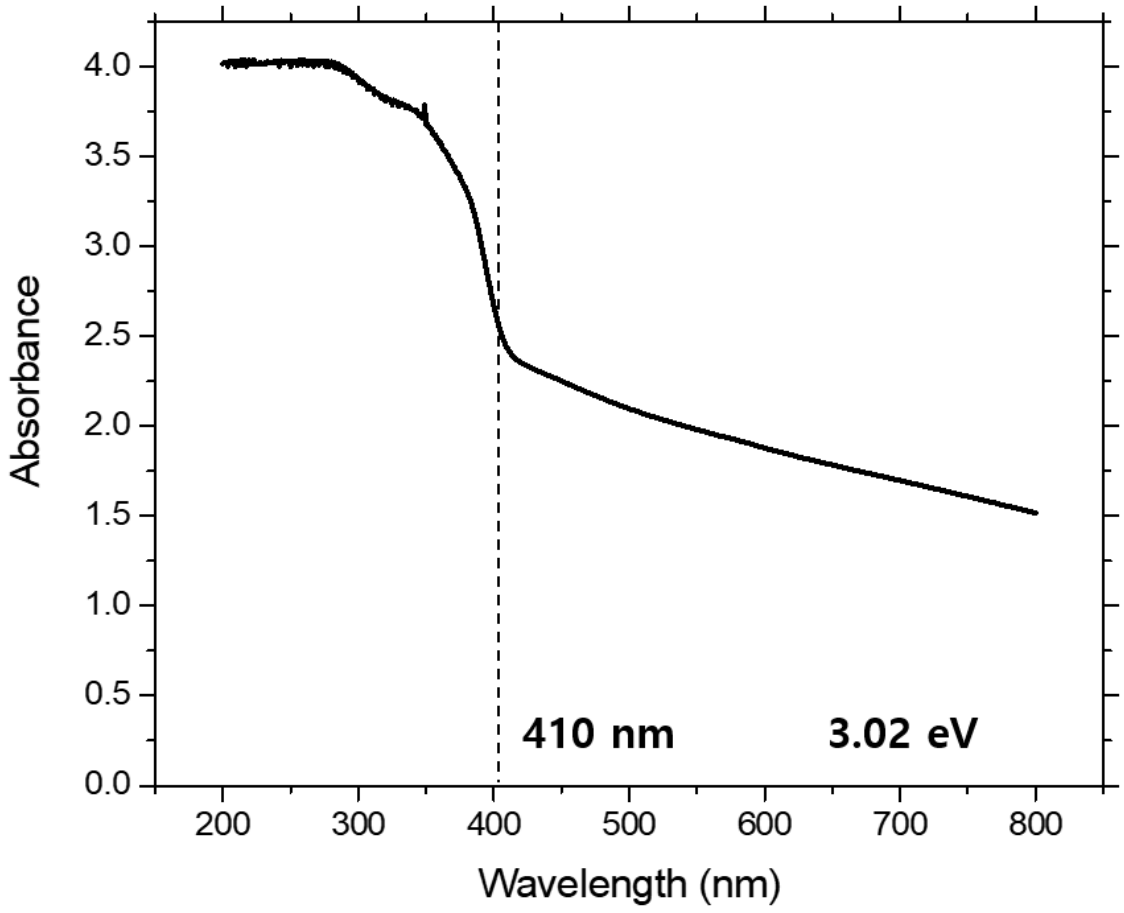

Figure 22. Absorbance of TiO_2 nanorods photoanode by using UV-Vis

And we also examined the morphology by scanning electron microscopy (SEM) technology. And we also confirmed that the uniform scales nanorods were grown through the SEM image (Figure 22). As you can see, the morphology of the nanorods, such as diameter, was uniformed, but verticality of TiO_2 nanorods was low. It has been reported because of the presence of the seeded layer (TiO_2 polymer Sol). The seeded layer progressed the verticality of TiO_2 nanorods.[77]

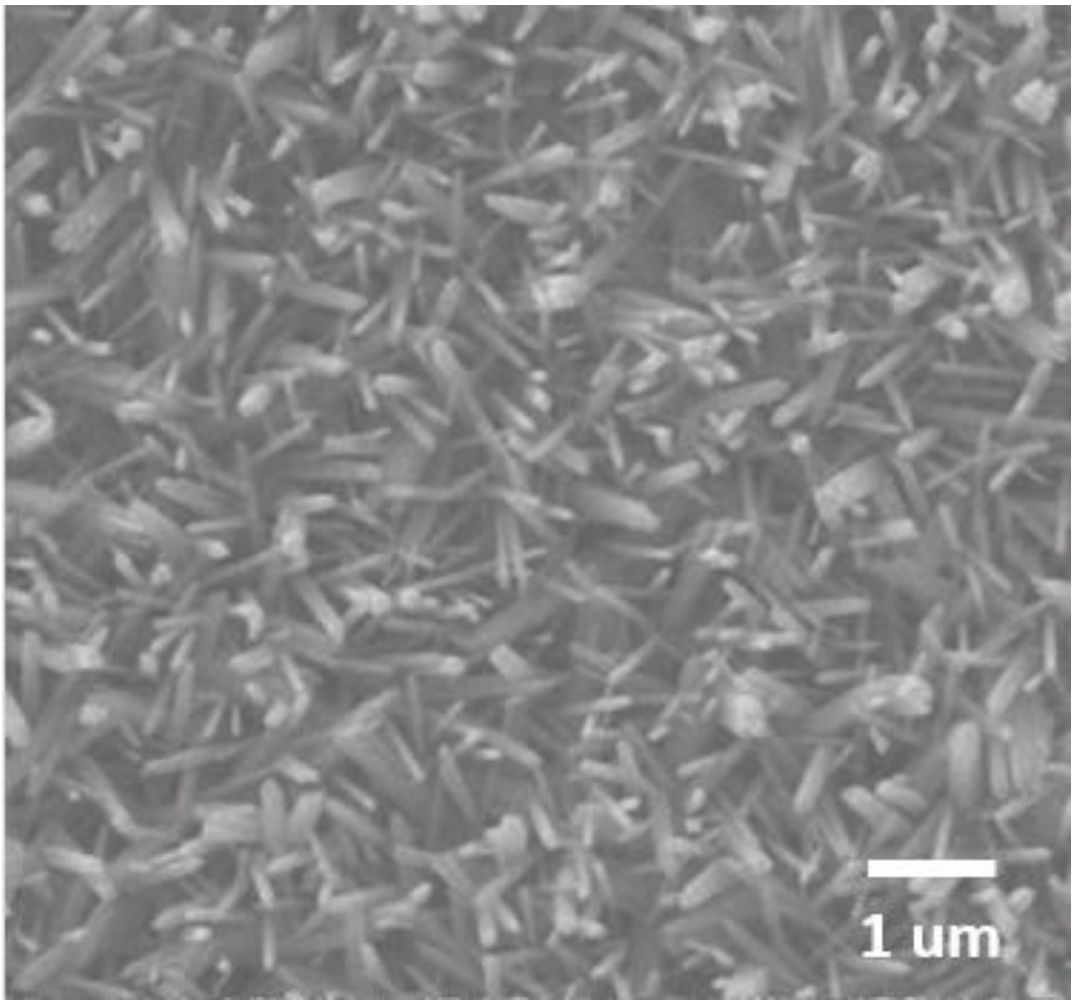

Figure 23. SEM image of TiO_2 nanorods photoanode with no seeded layer

We evaluated the photocurrent characterization of the TiO_2 nanorods photoanode itself in seawater.

Linear Sweep Voltammetry measurement was performed by using 3-electrode configuration using Ag/AgCl 3M NaCl reference electrode and Pt wire counter electrode (Figure 23).

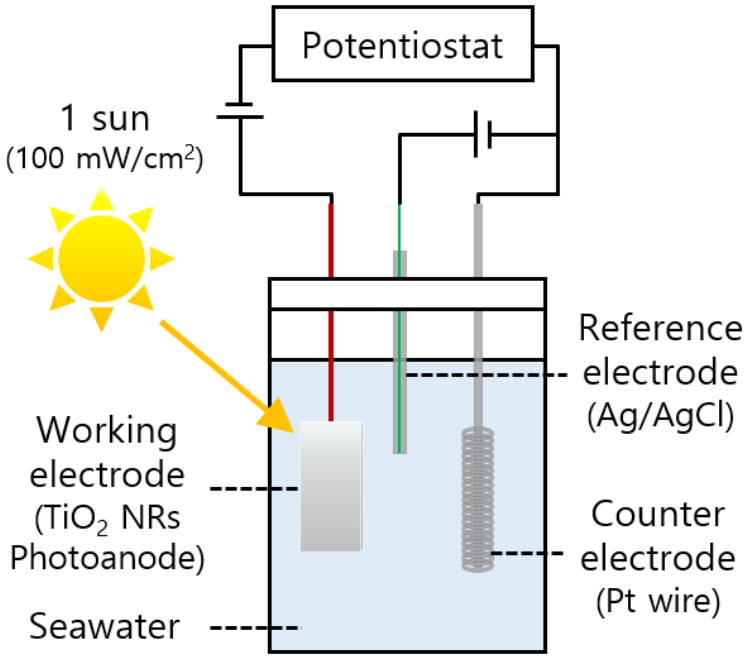

Figure 24. Schematic of 3-electrode configuration with TiO_2 nanorods photoanode working electrode, Ag/AgCl 3M NaCl reference electrode, and Pt wire counter electrode

As a result, we confirmed that no photocurrent was generated under the dark condition up to a high potential of 2.0 V_{RHE}, and 0.78 mA/cm^2 of photocurrent was observed at 1.23 V_{RHE} under 1 sun condition (100 mW/cm^2). It means that the TiO_2 nanorods photoelectrode can only generate photocurrent when it receives the solar energy. Under chopped light illumination, we confirmed that the generation of photocurrent due to the presence of light changes rapidly. This result suggests that the activity and stability of TiO_2 nanorods photoanode are high (Figure 24).

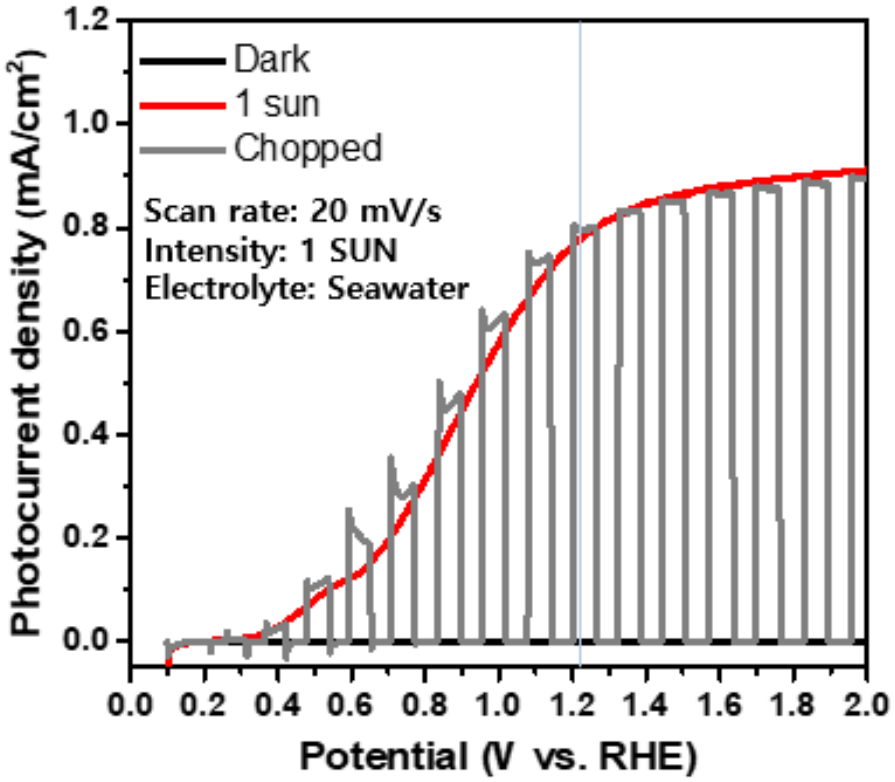

Figure 25. The I-V curves of TiO_2 nanorods photoanode with 3-electrode configuration under dark state, 1 sun condition and chopped condition

2.7. Performance of Solar seawater battery

To evaluate the photocurrent performance of the TiO_2 nanorods photoanode in the solar seawater battery, we performed Linear Sweep Voltammetry measurement by using the 2-electrode configuration (Figure 25).

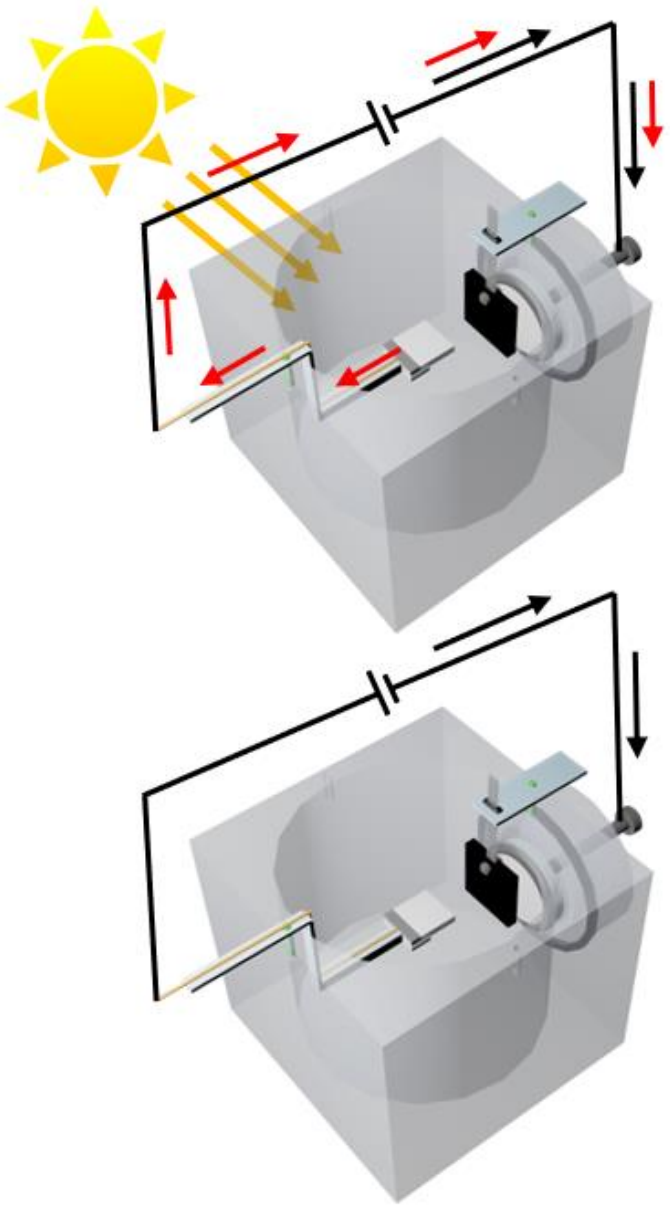

Figure 26. Schematic of 2-electrode configuration with TiO_2 nanorods photoanode working electrode and seawater coin-type cell counter electrode

As a result, we confirmed that no photocurrent was generated under the dark condition, and 0.44 mA/cm^2 of photocurrent was observed at 3.48 V vs Na/Na$^+$ under 1 sun condition, and the onset potential was 2.5 $V_{Na/Na+}$ (Figure 26).

We confirmed that the TiO_2 nanorods photoanode can generated the photocurrent at the voltage (2.5 $V_{Na/Na+}$) lower than the theoretical voltage of OER / ORR (3.48 $V_{Na/Na+}$) through the input of solar energy.

This is not possible with an electrocatalyst using kinetic. This means that the voltage efficiency can be increased through a thermodynamically favorable method using a TiO_2 nanorods photoanode.

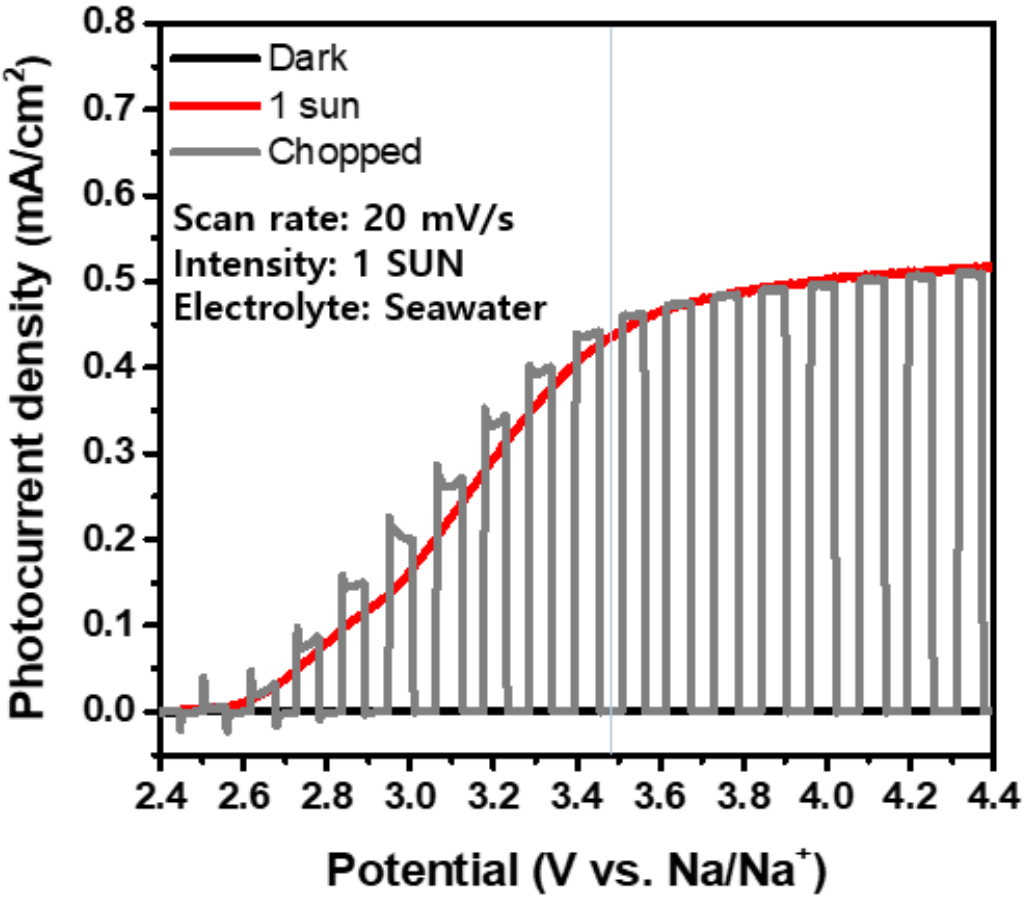

Figure 27. The I-V curves of TiO_2 nanorods photoanode with seawater coin-type cell under dark state, 1 sun condition and chopped condition

To confirm that the seawater cell can be charged stably for a long time using the TiO_2 Nanorods photoanode, chronoamperometry measurement was performed with applied bias for 8 hours (Figure 27). The reason we set it to 8 hours is because it assumes a day. We confirmed that the photocurrent is generated constantly without any significant difference. And the inset I-V curves also remained unchanged before and after this stability test. These result mean that the solar seawater battery system is stable during the photo-charging process. Therefore, we investigated how much the charge voltage could be lowered using the TiO_2 Nanorods photoanode.

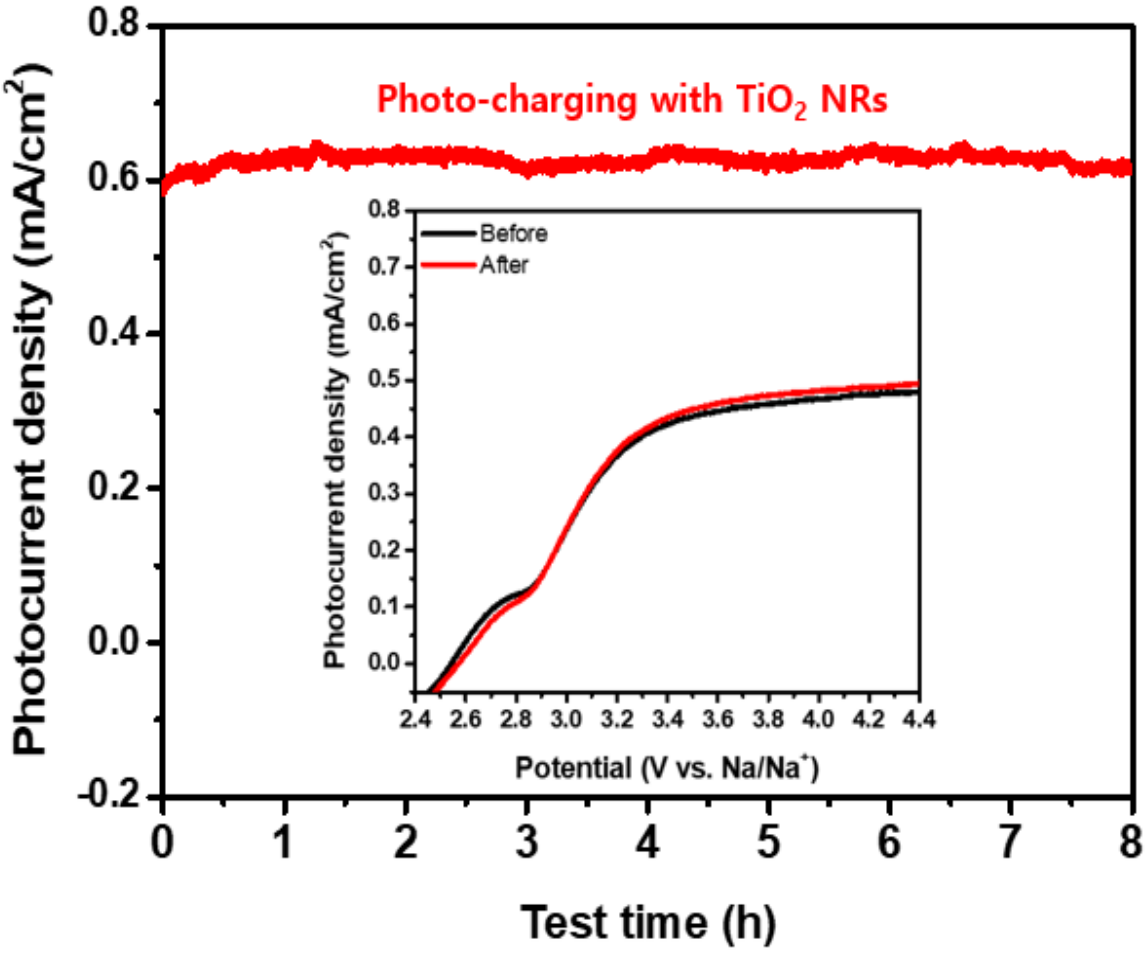

Figure 28. Chronoamperometry measurement of TiO_2 nanorods photoanode for checking long term stability

To confirm how much the charge voltage can be lowered, we compared the photo-charging possibility of the TiO_2 Nanorods photoanode and heated carbon felt.

The test was performed at 0.01 mA/cm^2 under the dark and 1 Sun condition for 1 minute each (Figure 28).

When we charged with the heated Carbon Felt, the charging voltage was generated without change regardless of the solar energy. In contrast to the heated carbon felt, for the TiO_2 Nrs photoanode, the charging was performed at a high voltage of ~4.8 V under the dark condition because there is no solar energy. But the photo-charging voltage was reduced to ~2.6 V under 1 sun condition. As a result, we concluded that the photo-charging voltage can be lowered effectively.

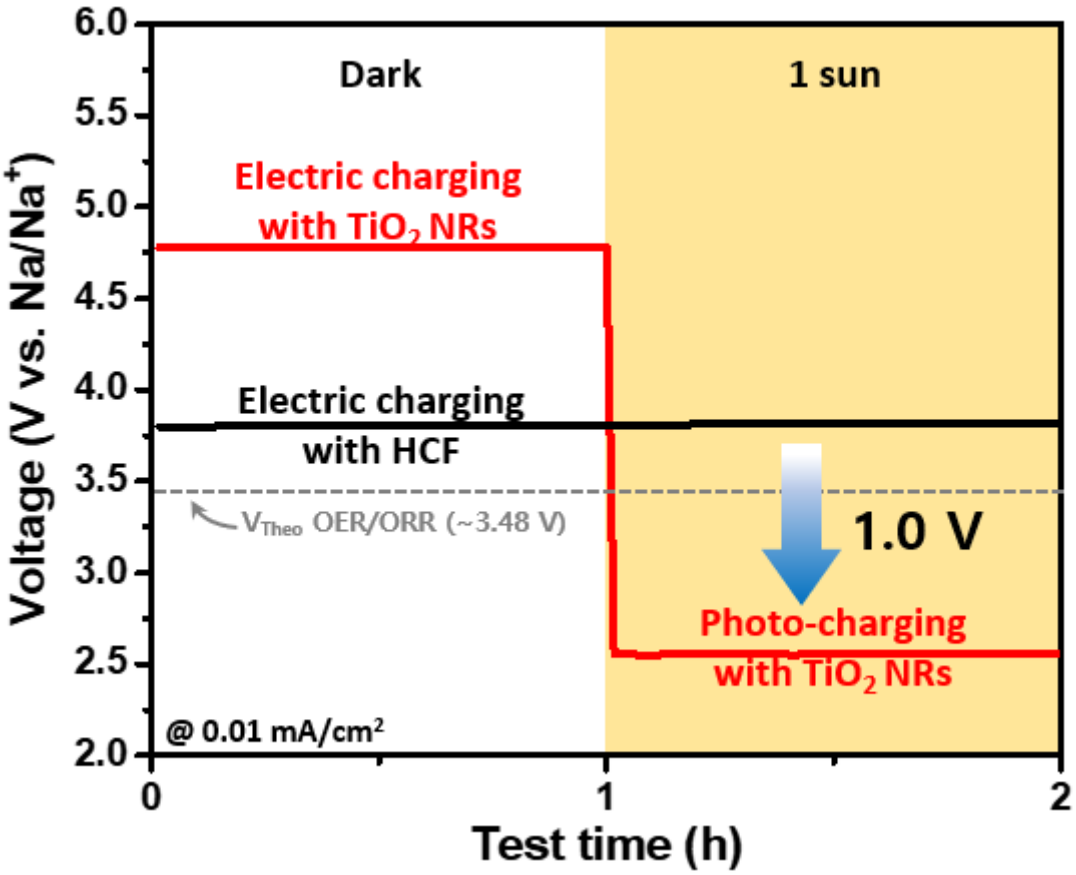

Figure 29. Charging curves with heated carbon felt and TiO_2 nanorods photoanode under the dark state and 1 sun condition for 1 minute each

We carried out the charging and discharging process under the condition of 0.1 mA/cm^2 for 8 hours (Figure 29).

The existing seawater battery with the heated carbon felt was charged at ~3.8 V and discharged at ~2.6 V.

Under illumination, photo-charging was performed at ~2.6 V with the photoanode, and the discharging voltage was ~2.8 V with the heated carbon felt in solar seawater battery.

So, we confirmed that the voltage efficiency increases from 74 % to 108 % at 0.1 mA/cm^2. It is noticeable that the charging voltage is lower than the discharging voltage, which is impossible thermodynamically without the solar energy input.

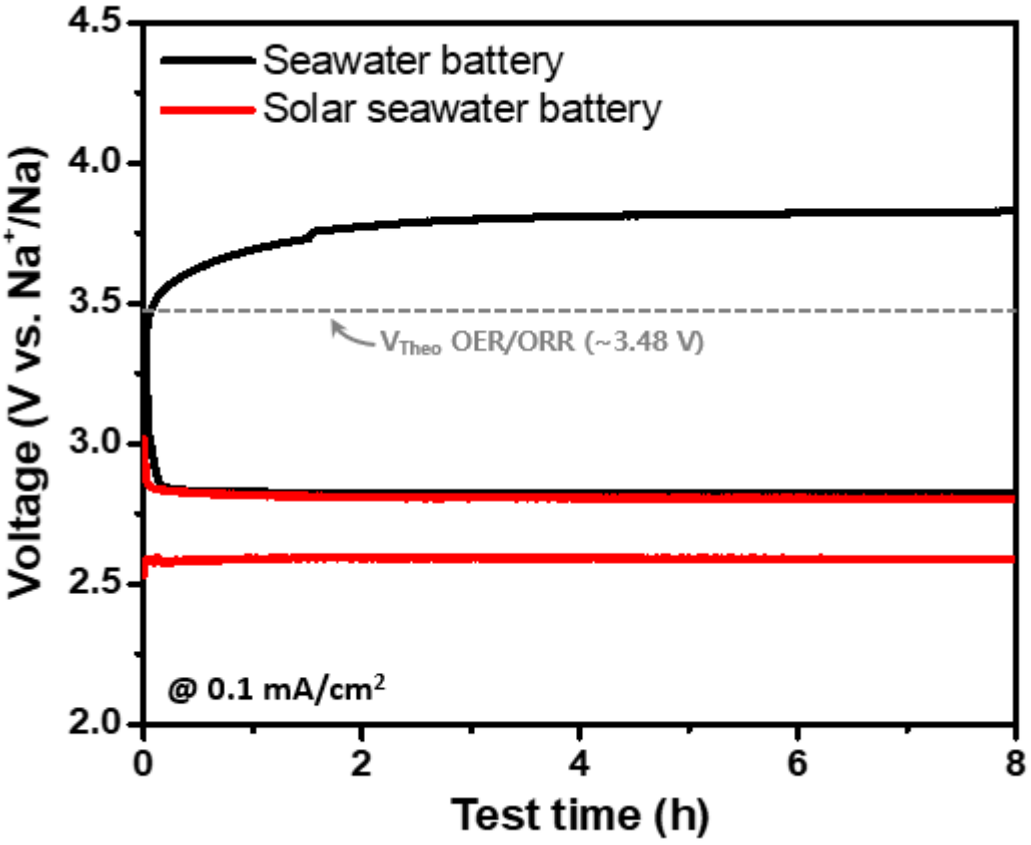

Figure 30. Voltage profile of seawater battery and solar seawater battery

We also performed the cycling performance of the solar seawater battery (Figure 30).

As mentioned before, Galvanostatic cycling tests performed on solar seawater battery used two channels to decouple and independently cycle the OER and ORR electrodes.

We further examined cycling performance at 0.1 mA/cm^2 for 8 h each. The cell cycled stably with a photo-charge voltage of ~2.6 V and a discharge voltage of ~2.8 V for 10 cycles (total 160 h), showing an average voltage efficiency of 108 %. This indicates that the solar seawater battery could achieve the stable solar charge of the seawater cell with increased voltage efficiency.

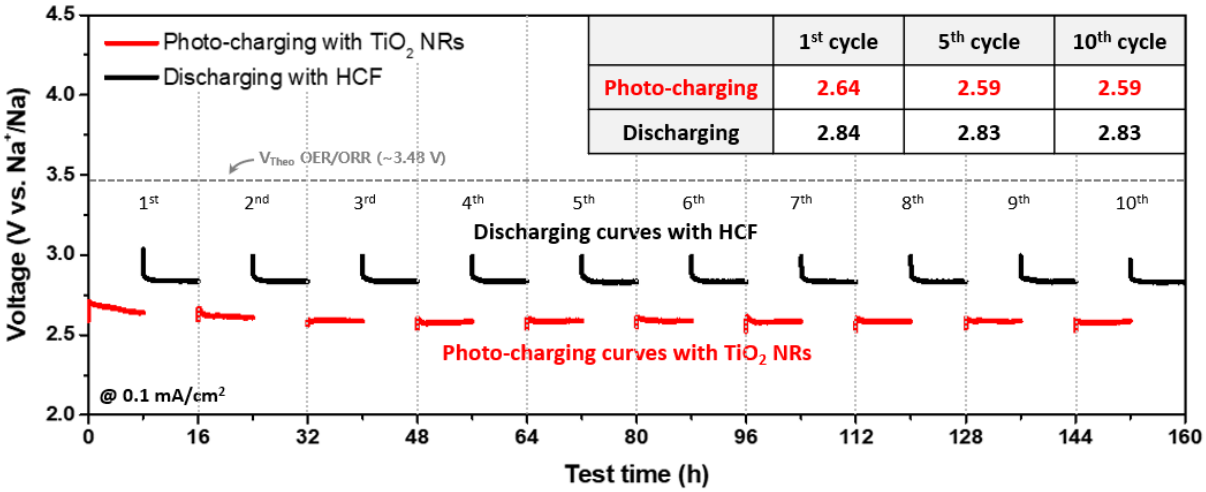

	1st cycle	5th cycle	10th cycle
Photo-charging	2.64	2.59	2.59
Discharging	2.84	2.83	2.83

Figure 31. Cycle performance of solar seawater battery

3. Experimental

3.1. Preparation of TiO_2 nanorods on FTO

First, we washed FTO substrate for 10 min using an ultrasonicator in a mixed solution. Second, Titanium n-butoxide (KANTO chem.) was added into an aqueous HCl solution under magnetic stirring. Third, after stirring, the solution was poured into a Teflon-lined stainless-steel autoclave and FTO substrate was immersed in the solution. Fourth, the stainless-steel autoclave was sealed and heated in an oven at 150 C for 5 hours without stirring. Lastly, after heating, the obtained product was washed with DI (deionized) water and annealed at 450 °C for 1 hour in the air. [77]

3.2. Preparation of cathode current collector

Carbon felts (3 mm soft felt (PAN-based), CNF Co. Ltd) were used as the current collector for seawater battery. The thickness and electrical resistance were around 3.0 mm and 0.20 ~ 0.25 Ω cm^2, respectively. Before use, carbon felts were heating for the hydrophilicity of the surface at 500 °C in the speed of 5 °C min−1) for 2 h in ambient air condition.

4. Conclusion

By benchmarking the solar rechargeable battery, we designed the solar seawater battery (SSB) which integrates TiO_2 nanorods photoanode and the seawater battery (SWB) into a single device to solve the low voltage efficiency issue of the SWB. In the SSB, NASICON ($Na_3Zr_2Si_2PO_{12}$) serves as the solid electrolyte. Aqueous (seawater) and non-aqueous liquid electrolytes, which are identical to those in the SWB, also are utilized. The cathodes are composed of two decoupled electrodes, TiO_2 nanorods photoanode and heated carbon felt (HCF), for OER and ORR, respectively. Then, to implement the SSB system practically, we designed the SSB tester optimized for the cell design and configuration.

During the photo-charging process of the SSB, the photo-generated holes of the valence band transfer to the Photoanode/seawater interface, oxidizing seawater to O_2. Meanwhile, the photo-excited electrons of the conduction band transfer to the anode through the external circuit, reducing the Na ions to Na metal, and the generated photovoltage is utilized to compensate the required charging voltage.

The voltage efficiency of the SWB was ~74 %. By utilizing the solar energy, the photo-assisted charging of the SSB was ~2.6 V, which is lower than its discharging voltage of ~2.8 V. The voltage efficiency of the SSB was ~108%. This result presented that the voltage efficiency was increased by ~34% compared to that of the SWB through a thermodynamically favorable method by using the TiO_2 nanorods photoanode.

For the higher voltage efficiency of the SSB, it is important to enhance the PEC performance of TiO_2 nanorods photoanode. Therefore, Further direction on the PEC performance of TiO_2 nanorods photoanode is to improve with doping and/or sensitization for better charge carrier separation and collection properties. Among various candidates, photoanode materials with smaller bandgap than TiO_2, such as WO_3 and $BiVO_4$, can be used to further increase voltage efficiency.

5. Reference

[1] Z. Yang, J. Zhang, M. C. W. Kintner-Meyer, X. Lu, D. Choi, J. P. Lemmon, J. Liu, Chem Rev. 2011, 111. 3577.

[2] R. C. Armstrong, C. Wolfram, K. P. de Jong, R. Gross, N. S. Lewis, B. Boardman, A. J. Ragauskas, K. Ehrhardt-Marinez, G. Crabtree, M. V. Ramana, Nat. Energy 2016, 1, 15020.

[3] M. Z. Jacobson, M. A. Delucchi, Z. A. F. Bauer, S. C. Goodman, W. E. Chapman, M. A. Cameron, C. Bozonnat, L. Chobadi, H. A. Clonts, P. Enevoldsen, J. R. Erwin, S. N. Fobi, O. K. Goldstrom, E. M. Hennessy, J. Liu, J. Lo, C. B. Meyer, S. B. Morris, K. R. Moy, P. L. O'Neill, I. Petkov, S. Redfern, R. Schucker, M. A. Sontag, J. WQang, E. Weiner, A. S. Yachanin, Joule 2017, 1, 108.

[4] S. Chu, Y. Cui, N. Liu, Nat. Mater. 2017, 16, 16.

[5] H. J. Snaith, L. Schmidt-Mende, Adv. Mater. 2007, 19, 3187.

[6] B. C. Thompson, J. M. J. Frechet, Angew. Chem. Int. Ed. 2008, 47, 58.

[7] T. Chen, L. Qiu, Z. Cai, J. Ren, H. Li, H. Lin, X. Sun, H. Peng, Angew. Chem. Int. Ed. 2012, 51, 11977.

[8] T. Song, B. Sun, ChemSusChem 2013, 6, 408.

[9] M. Graetzel, R. A. J. Janssen, D. B. Mitzi, E. H. Sargent, Nature 2012, 488, 304.

[10] Q. Schiermeier, J. Tollefson, T. Scully, A. Witze, O. Morton, Nature 2008, 454, 816.

[11] N. S. Lewis, Science 2007, 315, 798.

[12] Solar and wind are coming. And the power sector isn't ready. http https://www.vox.com/energy-and-environment/2018/5/18/17359730/wind-solar-power-grid-electricity-managers.

[13] Energy storage could be a game-changer for renewable energy. https://www.qic.com.au/knowledge-centre/technology-disruptions-affecting-infrastructure-20160414.

[14] O. Schmidt, A. Hawkes, A. Gambhir, I. Staffell, Nat. Energy 2017, 2, 17110.

[15] D. Larcher, J-M. Tarascon, Nat. Chem. 2015, 7, 19.

[16] B. D. McCloskey, J. Phys. Chem. Lett. 2015, 6, 3592.

[17] The cost components of a lithium ion battery. https://qnovo.com/82-the-cost-components-of-a-

battery/.

[18] Nano One is Redefining Battery Grade Lithium. https://nanoone.ca/nano-one-redefining-battery-grade-lithium/.

[19] J. K. Kim, F. Mueller, H. Kim, J. S. Park, D. H. Lim, G. T. Kim, D. Bresser, S. Passerini, Y. Kim, NPG Asia Mater. 2014, 6, e144.

[20] H. Kim, J. S. Park, S. H. Sahgong, S. Park, J. K. Kim, Y. Kim, J. Mater. Chem. A 2014, 2, 19584.

[21] Y. I. Kim, H. Kim, S. Park, I. Seob, Y. Kim, Electrochim Acta 2016, 191, 1.

[22] J. K. Kim, F. Mueller, H. Kim, S. Jeong, J. S. Park, S. Passerini, Y. Kim, ChemSusChem 2016, 9, 42.

[23] S. Park, B. SenthilKumar, K. Kim, S. M. Hwang, Y. Kim, J. Mater. Chem. A 2016, 4, 7207.

[24] J. I. Jung, D. Kim, H. Kim, Y. N. Jo, J. S. Park, Y. Kim, ACS Appl. Mater. Interfaces 2017, 9, 304.

[25] J. H. Han, S. M. Hwang, W. S. Go, S. T. Senthilkumar, D. Jeon, Y. Kim, J. Power Sources 2018, 374, 24.

[26] S. Jeong, S. H. Sahgong, J. H. Kim, S. M. Hwang, Y. Kim, H. R. Moon, J. Mater. Chem. A 2016, 4, 13468.

[27] M. Abirami, S. M. Hwang, J. Yang, S. T. Senthilkumar, J. Kim, W. S. Go, B. Senthilkumar, H. K. Song, Y. Kim, ACS Appl. Mater. Interfaces 2016, 8, 32778.

[28] S. T. Senthilkumar, S. O. Park, J. Kim, S. M. Hwang, S. K. Kwak, Y. Kim, J. Mater. Cem. A 2017, 5, 14174.

[29] D. H. Suh, S. K. Park, P. Nakhanivej, Y. Kim, S. M. Hwang, H. S. Park, J. Power Sources 2017, 372, 31.

[30] K. Kim, S. M. Hwang, J. S. Park, J. H. Han, J. Kim, Y. Kim, J. Power Sources 2016, 313, 46.

[31] S. T. Senthilkumar, M. Abirami, J. Kim, W. S. Go, S. M. Hwang, Y. Kim, J. Power Sourves 2017, 341, 404.

[32] P. Manikandan, K. Kishor, J. H. Han, Y. Kim, J. Mater. Chem. A 2018, 6, 11012.

[33] S. M. Hwang, J. Kim, Y. I. Kim, Y. Kim, J. Mater. Chem. A 2016, 4, 17946.

[34] Y. I. Kim, J. K. Kim, C. Vaalma, G. H. Bae, G. T. Kim, S. Passerini, Y. Kim, Carbon 2018, 129, 564.

[35] Y. I. Kim, S. M. Hwang, H. I. Yu, Y. Kim. J. Mater. Chem. A 2018, 6, 3046.

[36] Y. Zhang, S. T. Senthilkumar, J. S. Park, J. H. Park, Batteries Supercaps 2018, 1, 1.

[37] Y. I. Kim, G. T. Kim, S. Jeong, X. Dou, C. Geng, Y. Kim, S. Passerini, Energy Storage Mater. 2019, 16, 56.

[38] S. M. Hwang, J. S. Park, Y. I. Kim, W. S. Go, J. H. Han, Y. J. Kim, Y. Kim, Adv. Mater. 2018, 1804936.

[39] Structure and performance of seawater battery. http://www.4toone.com/main/?skin=sub2_1.html

[40] Key World Energy Statistics 2013. International Energy Agency, Paris, 2013

[41] J. P. Holdren, Energy and sustainability. Science 315, 737 (2007)

[42] J. G. Mavroides, J. A. Kafalas, D. F. Kolesar, Appl. Phys. Lett. 28 (1976) 241-243.

[43] T. Watanabe, A. Fujishima, K. i. Honda, Bull. Chem. Soc. Jpn. 49 (1976) 355-358.

[44] M. S. Wrighton, A. B. Ellis, P. T. Wolczanski, D. L. Morse, H. B. Abrahamson, D. S. Ginley, J. Am. Chem. Soc. 98 (1976) 2774-2779.

[45] T. Hisatomi, J. Kubota, K. Domen, Chem. Soc. Rev., 43 (2014), pp. 7520-7535

[47] X. Shi, L. Cai, M. Ma, X. Zheng, J.H. Park, ChemSusChem, 8 (2015), pp. 3192-3203

[48] N.S. Lewis J., Electroanal. Chem., 508 (2001), pp. 1-10

[49] B.D. Alexander, P.J. Kulesza, I. Rutkowska, R. Solarska, J. Augustynski J., Mater. Chem., 18 (2008), pp. 2298-2303

[50] K. Maeda, K. Domen, J. Phys. Chem. Lett., 1 (2010), pp. 2655-2661

[51] T. Wang, Z. Luo, C. Li, J. Gong, Chem. Soc. Rev., 43 (2014), pp. 7469-7484

[52] K.T. Fountaine, H.J. Lewerenz, H.A. Atwater, Nat. Commun., 7 (2016), p. 13706

[53] L.M. Peter J., Solid State Electrochem., 17 (2012), pp. 315-326

[54] I. Roger, M.A. Shipman, M.D. Symes, Nat. Rev. Chem., 1 (2017), p. 0003

[55] J. Gu, J.A. Aguiar, S. Ferrere, K.X. Steirer, Y. Yan, C. Xiao, James L. Young, M. Al-Jassim, N.R.

Neale, J.A. Turner, Nat. Energy, 2 (2017), p. 16192

[56] B.H. Simpson, J. Rodríguez-López, Anal. Methods UK, 7 (2015), pp. 7029-7041

[57] P. Migowski, A.F. Feil, Recycl. Catal., 3 (2016), pp. 1-12

[58] M.R. Nellist, F.A. Laskowski, F. Lin, T.J. Mills, S.W. Boettcher, Acc. Chem. Res., 49 (2016), pp. 733-740

[59] R. Abe, J. Photochem. Photobiol. C Photochem. Rev., 11 (2010), pp. 179-209

[60] S.T. Kochuveedu, J. Nanomater., 2016 (2016), pp. 1-12

[61] L.M. Peter, Chem. Rev., 90 (1990), pp. 753-769

[62] A.G. Tamirat, J. Rick, A.A. Dubale, W.-N. Su, B.-J. Hwang, Nanoscale Horiz., 1 (2016), pp. 243-267

[63] S. Chen, S.S. Thind, A. Chen, Electrochem. Commun., 63 (2016), pp. 10-17

[64] 5. K. Sivula, R. van de Krol, Semiconducting materials for photoelectrochemical energy conversion Nat. Rev. Mater. 1, 15010 (2016).

[65] M. A. Pellow, C. J. M. Emmott, C. J. Barnhart, S. M. Benson, Hydrogen or batteries for grid storage? A net energy analysis Energy Environ. Sci. 8, 1938-1952 (2015).

[66] S. Kurtz, N. Haegel, R. Sinton, R. Margolis, A new era for solar Nat. Photon. 11, 3-5 (2017).

[67] J. Cen, Q. Wu, M. Liu, A. Orlov, Green Energy & Environment 2 (2017) 100-111

[68] H.Ahmad, S.K.Kamarudin, L.J.Minggu, M.Kassima, Renewable and Sustainable Energy Reviews 43 (2015) 599–610

[69] M. G. Walter, E. L. Warren, J. R. McKone, S. W. Boettcher, Q. Mi, E. A. Santori, N. S. Lewis, Chem. Rev. 2010, 110, 6446–6473

[70] P. He, T. Zhang, J. Jiang, H. Zhou, J. Phys. Chem. Lett. 2016, 7, 1267;

[71Mark K. Debe, Nature 2012, 486, 43;

[72] Y. Lee, J. Suntivich, K. J. May, E. E. Perry, Y. Shao-Horn, J. Phys. Chem. Lett. 2012, 3, 399;

[73] B. P. Setzler, Z. Zhuang, J. A. Wittkopf, Y. Yan, Nat. Nanotechnol. 2016, 11, 1020.

[74] Q. Li, N. Li, M. Ishidab. H. Zhou, J. Mater. Chem. A, 2015, 3, 20903

[75] D. Schmidt , M. D. Hager , U. S. Schubert, Adv. Energy Mater. 2016, 6, 1500369

[76] W. Li, H.-C. Fu, L. Li, M. Cabán-Acevedo, J.-H. He, S. Jin, Integrated Photoelectrochemical Solar Energy Conversion and Organic Redox Flow Battery Devices Angew. Chem. Int. Ed. 55, 13104-13108 (2016).

[77] S. Liao, X. Zong, B. Seger, T. Pedersen, T. Yao, C. Ding, J. Shi, J. Chen, C. Li, Integrating a dual-silicon photoelectrochemical cell into a redox flow battery for unassisted photocharging Nat. Commun. 7, 11474 (2016).

[78] Q. Cheng, W. Fan, Y. He, P. Ma, S. Vanka, S. Fan, Z. Mi, D. Wang, Photorechargeable High Voltage Redox Battery Enabled by Ta3N5 and GaN/Si Dual-Photoelectrode Adv. Mater. 29, 1700312 (2017).

[79] G. Nikiforidis, K. Tajima, H. R. Byon, High Energy Efficiency and Stability for Photoassisted Aqueous Lithium–Iodine Redox Batteries ACS Energy Lett. 1, 806-813 (2016).

[80] Y. Liu, N. Li, K. Liao, Q. Li, M. Ishida, H. Zhou, Lowering the charge voltage of Li-O2 batteries via an unmediated photoelectrochemical oxidation approach J. Mater. Chem. A 4, 12411-12415 (2016).

[81] Renewable Energy World news report, 100 GW of Solar PV Now Installed in the World Today, http://www.renewableenergyworld.com/rea/news/article/2013/02/100-gw-of-solar-pv-now-installed-inthe-world-today (accessed February 2015).

[82] a) K. Wang, H. Wu, Y. Meng, Y. Zhang, Z. Wei, Energy Environ. Sci. 2012, 5, 8384;

[83] L. Li, Z. Wu, S. Yuan, X.-B. Zhang, Energy Environ. Sci. 2014, 7, 2101.

[84] P. Liu, H. Yang, X. Ai, G. Li, X. Gao, Electrochem. Commun. 2012, 16, 69.

[85] Z. Yang, L. Li, Y. Luo, R. He, L. Qiu, H. Lin, H. Peng, J. Mater. Chem. A 2012, 1, 954.

[86] Y. Li, J. Z. Zhang, Laser Photonics Rev. 4, No. 4, 517–528 (2010)

Acknowledgement

지난 2년간 울산에서 좋은 환경과 좋은 사람들 덕분에 잊지못할 추억을 남겼습니다. 많은 분들의 도움으로 2년 간의 학위기간동안 행복하게 연구하며 많은 성장을 이룰 수 있었습니다.

우선, 정말 부족했던 저에게 기회를 주시고, 주체적인 연구자의 길로 이끌어주고 계시는 김영식 지도교수님께 깊은 감사를 드립니다. 석사 학위 기간 동안의 교수님 가르침을 잊지 않고 앞으로도 계속해서 발전하여 훌륭한 제자가 될 수 있도록 항상 노력하겠습니다.

또한, 바쁘신 중에도 학위논문 심사를 맡아 주시고 아낌없는 조언을 주신 최윤석 교수님, 장지욱 교수님께도 깊은 감사를 드립니다.

그리고 아무것도 모르던 저에게 관심을 가져 주시고 연구에 대한 자세 등 정말 많은 것에 대해 고민하고 발전하도록 도와 주신 황수민 박사님께 깊은 감사를 드립니다.

2년 동안 동고동락한 YK group 선후배님들 정말 감사드립니다. 우선, 지금은 박사가 되어 랩실을 떠나신 사수 진협이형께 정말 감사드립니다. 정말 많은 것을 배울 수 있었습니다. 그리고 곧 떠나실 항상 학생들에게 도움될 만한 논문을 알려주시는 용일이형, 같은 시기에 입학해서 많은 걸 알려주고 있으신 영진이형, 석사 입학 준비 많이 도와주고 랩실의 막내 역할 마친 영재, 랩실의 비타민 역할을 하는 입학 동기 다송, 여자친구 만나고 행복을 찾은 랩장 영준, 이 시대의 진정한 사랑꾼 유부남 현태, 담수화 이끌고 있는 몸짱 남혁, 양극팀에서 배우고 있는 외국인 원석이, 주위 의식 많이 하는 엉뚱한 세영이, 물어볼 때마다 친절히 알려주는 박학다식 우석이, 연구 외적으로 힘들 때마다 정말 큰 도움이 되어주고 내로남불 싫어하는 동갑 친구 현우, 마지막으로 처음 들어올 때부터 연구뿐 아니라 연구 외적으로도 정말 많은 걸 알려줘 석사 생활을 무사히 잘 마칠 수 있도록

물심양면으로 도와준 알파고 정선이에게 정말 감사드립니다.

지금은 미국 가 있는 전 양극 팀장 제희, 졸업 전에도 자주 놀았고 석사 졸업하고도 자주 놀러와 주고 스트레스 해소해주는 혜인이도 정말 감사합니다. 이렇게 좋은 사람들 곁에서 실험실 생활 할 수 있어 정말 큰 행운이었고, 행복했습니다. 모두들 열심히 노력하시는 만큼 좋은 결과 있을 것이라 믿어 의심치 않습니다.

그리고 멀리 서울에서 타지 생활에 큰 즐거움을 주었던 친구들 모두 고맙다. 특히 재명, 주현, 재혁이 그리고 여기 있을 수 있도록 해준 민수. 정말 고맙고, 앞으로도 이 우정 변치 말자.

마지막으로, 사랑하는 우리 가족 정말 감사드립니다. 어머니, 아버지! 제가 부모님 밑에서 이렇게 잘 자라 사회에 필요한 사람이 되었습니다. 그 동안 바쁘고 멀다는 핑계로 집에 자주 찾아가지 못했는데, 이제는 보다 가까이에서 그동안의 은혜에 보답하며 살아갈 수 있도록 하겠습니다. 그리고 동생 현정이도 정말 고맙다. 지금까지도 잘 해줬지만 앞으로 더 잘 해줄게.

모두들 정말 감사드립니다.

2019년 7월

진호 올림